KAMONWAN KANPHAI

A THESIS SUBMITTED IN PARTIAL FULFILLMENT OF
THE REQUIREMENTS FOR MASTER DEGREE OF SCIENCE
IN CHEMISTRY
FACULTY OF SCIENCE
BURAPHA UNIVERSITY
2024

การพัฒนาฟิล์มพอลิเมอร์ชีวภาพที่มีองค์ประกอบของสารธรรมชาติออกฤทธิ์ทางชีวภาพสำหรับใช้ติดตามความสดของอาหาร

กมลวรรณ กันภัย

วิทยานิพนธ์นี้เป็นส่วนหนึ่งของการศึกษาตามหลักสูตรวิทยาศาสตรมหาบัณฑิต
สาขาวิชาเคมี
คณะวิทยาศาสตร์ มหาวิทยาลัยบูรพา
2567

DEVELOPMENT OF BIOPOLYMERIC BASED FILMS ENRICHED WITH BIOACTIVE NATURAL EXTRACT FOR FOOD FRESHNESS MONITORING

KAMONWAN KANPHAI

A THESIS SUBMITTED IN PARTIAL FULFILLMENT OF
THE REQUIREMENTS FOR MASTER DEGREE OF SCIENCE
IN CHEMISTRY
FACULTY OF SCIENCE
BURAPHA UNIVERSITY
2024

The Thesis of Kamonwan Kanphai has been approved by the examining committee to be partial fulfillment of the requirements for the Master Degree of Science in Chemistry of Burapha University

Advisory Committee

Principal advisor

Thanida R.

(Associate Professor Dr. Thanida Trakulsujaritchok)

Co-advisor

A. Athipornchai

(Assistant Professor Dr. Anan Athipornchai)

Examining Committee

Anyarat W. Principal examiner

(Assistant Professor Dr. Anyarat Watthanaphanit)

Piyaporn N. Member

(Assistant Professor Dr. Piyaporn Nanongkhai)

A. Athipornchai Member

(Assistant Professor Dr. Anan Athipornchai)

Thanida R. Member

(Associate Professor Dr. Thanida Trakulsujaritchok)

P. Usavadee Dean of the Faculty of Science

(Assistant Professor Dr. Usavadee Tuntiwaranuruk)

June 7, 2024

This Thesis has been approved by Graduate School Burapha University to be partial fulfillment of the requirements for the Master Degree of Science in Chemistry of Burapha University

Witawat Jangiam Dean of Graduate School

(Associate Professor Dr. Witawat Jangiam)

15 JULY 2024

65910112: MAJOR: CHEMISTRY; M.Sc. (CHEMISTRY)
KEYWORDS: κ-Carrageenan, Poly(vinyl alcohol), pH-sensitive film

KAMONWAN KANPHAI : DEVELOPMENT OF BIOPOLYMERIC BASED FILMS ENRICHEDWITH BIOACTIVE NATURAL EXTRACT FORFOOD FRESHNESS MONITORING. ADVISORY COMMITTEE: THANIDA TRAKULSUJARITCHOK, Ph.D. ANAN ATHIPORNCHAI 2024.

In this work, biopolymeric films of κ-carrageenan (KC)/poly(vinyl alcohol) (PV) were developed by a solution casting method. The optimization of composition between both homopolymers was done at ratios of 40:60, 50:50, and 60:40 κ-carrageenan:poly(vinyl alcohol). The swelling, solubility and moisture resistance of the fabricated films were studied and the results showed that the 40KC/60PV film exhibited outstanding properties. This film showed enhanced tensile strength and elongation at break compared to those of the 50KC/50PV and 60KC/40PV. In order to further improve the physicochemical properties of the film, the organic-inorganic crosslinked films using a siloxane crosslinker were fabricated through a sol-gel process. Investigation on the mechanical properties and swelling ability of the developed hybrid films showed significant improvement in their properties through covalent crosslinking between organic and inorganic networks. Therefore, the crosslinked film was modified for pH-sensitive applications by incorporating various amounts of crude extract obtained from *Ruellia squarrosa* (Fenzi) Cufod. flowers. The crude extract was rich in various bioactive compounds and capable of color change under different pH conditions. The pH-sensitive films were characterized using ATR-FTIR and SEM-EDX, thermal analysis, mechanical and UV–vis light barrier properties. The intermolecular interaction and compatibility of the crosslinked films incorporated with the crude extract were confirmed by ATR-FTIR and SEM-EDX. Incorporation of the crude extract enabled great improvement in water resistance, thermal stability, UV barrier performance and elongation at break, while a slight decrease in tensile strength at break was revealed. Additionally, the color changes of the pH-sensitive films were observed when exposed to volatile ammonia and immersed in varying pH solutions. The pH-sensitive films showed biodegradability with deteriorated in surface morphology and

weight loss over 60 days under the soil burial test. The pH-sensitive films possessed potential use in freshness monitoring application of fresh food tested with shrimp samples at room temperature. The film displayed distinct changes from pale yellow to green along with the spoilage of shrimps. Therefore, incorporation of the crude extract in the hybrid pH-sensitive κ-carrageenan/poly(vinyl alcohol) films exhibit strong potential for application in real-time food freshness monitoring.

ACKNOWLEDGEMENTS

This thesis has been an achievement with powerful support from my thesis advisor, Associate Professor Dr. Thanida Trakulsujaritchok. My deepest thanks to her, whose invaluable insights and guidance from day one to the successful completion of the thesis were instrumental in shaping this work. I also would like to extend my deep and sincere appreciation to my co-advisor, Assistant Professor Dr. Anan Athipornchai, who played a major role in guiding and supporting me throughout this thesis journey

I am also most grateful to the examination committee members, Assistant Professor Dr. Piyaporn Na Nongkhai and Assistant Professor Dr. Anyarat Watthanaphanit whose expertise and guidance were critical in the correction and improvement of this thesis.

I would like to thank all my lecturers and the scientist staff at the Department of Chemistry, Faculty of Science, Burapha University for their dedication to academic excellence which has been a constant source of motivation. I sincerely acknowledged the technical support provided by the Department of Chemistry, Faculty of Science, Burapha University

Financial support from the Center of Excellence for Innovation in Chemistry (PERCH-ICI), Ministry of Higher Education, Science, Research and Innovation is gratefully acknowledged.

This work was supported by the Science Innovation Facility, Faculty of Science, Burapha University (SIF-IN-65910112).

Finally, a huge thank you to my family for all their enduring support and encouragement throughout the journey of my study. Their belief in me provided the motivation to persevere during challenging periods. I am truly thankful to my friends and everyone who have been a source of support and joy throughout this thesis project.

Kamonwan Kanphai

TABLE OF CONTENTS

Page

LIST OF TABLES

Page

LIST OF FIGURES

Page

CHAPTER 1
INTRODUCTION

1.1 Background

Food packaging is one of the most important items to hold food safety during storage and marketing. Typically, food packaging are utilized for marketing purpose to attract consumer attention, showing food information concerning nutritional fact and shelf-life and protecting the food quality (Sharma, Barkauskaite, Jaiswal, & Jaiswal, 2021).

Recently, smart polymeric materials have been widely explored for the application of food packaging and considered as the alternative to protect the quality and increase the shelf-life of packaged foods due to their potential characters in quality control, shelf-life monitoring, and antioxidant activity (Fortunati et al., 2018). The interest in smart materials containing natural pH indicator and bioactive substances (such as antimicrobial and antioxidant compounds) has been increased for alternatives to benefit both environment and consumer's health (Sharma et al., 2021). A number of research have reported on the utilization of natural extracts containing anthocyanins for the purpose of active packaging in the field of pH-sensitive packaging for detection of food freshness (Zhao, Liu, Zhao, & Wang, 2022). Natural compounds such as anthocyanins have been reported as pH indicator in the blends of biopolymers including chitosan, carrageenan and pectin for food packaging application. The fabrication of films based on chitosan and nanosized TiO_2 for multifunctional food packaging (e.g. antioxidant, antimicrobial, ethylene scavenging and pH-sensitive properties) containing anthocyanin from black plum peel extract has been investigated. Natural compounds obtained from sweet potato, hibiscus, pomegranate seed, purple cabbage and butterfly pea flower have been reported to possess pH indicator property (Zhao et al., 2022). In our preliminary research, we have found that the ethanol extract of *Ruellia squarrosa* (Fenzi) Cufod. flower has an outstanding characteristic of color changing with pH and can be incorporated in polymeric packaging film to produce a smart material with freshness monitoring property

Utilization of smart polymeric films has gained significant attention in the food industry especially those with non-toxicity, renewability, and environmental friendliness properties derived from biopolymers such as starch, cellulose, chitin, chitosan, gelatin and carrageenan (Jamroz et al., 2021). Carrageenan, an anionic sulfonated polysaccharide, is a popular natural biopolymer obtained by extraction of red seaweeds. The structure of this biopolymer consists repeating units of α-(1→3)-D-galactose and β-(1→4)-3,6-anhydro-D- or L-galactose. Three types of carrageenan are kappa, iota and lambda depending on sulfate groups in structure. Carrageenan exhibits several properties including gel-forming, thickening and non-toxicity. They are widely used in drugs delivery system, pharmaceutical industry and food packaging industry (Park, Lee, Jung, & Park, 2001). Investigation on the use of *κ*-carrageenan as intelligent packaging films possessing antioxidant and pH-sensitive properties was performed by incorporation of mulberry polyphenolic extract containing anthocyanin (Y. Liu et al., 2019). The fabrication of *κ*-carrageenan films incorporated with curcumin for monitor the freshness of pork and shrimp was also reported (J. Liu et al., 2018). It has been generally known that carrageenan has drawbacks of high solubility and poor mechanical properties. In order to improve its weakness, blending carrageenan with other polymers has been explored. Poly(vinyl alcohol) produced by the hydrolysis of polyvinyl acetate is commonly used in food packaging industry due to its non-toxicity, good solubility in water, film-forming, flexibility and high mechanical properties. (Nagarkar, 2019). Literature reviews have reported on using poly(vinyl alcohol) blend films for freshness monitoring of foods such as the films containing curcumin with pH sensing property (J. Liu et al., 2018), red cabbage anthocyanins/poly(vinyl alcohol)/sodium carboxymethyl cellulose colorimetric films for pork freshness monitoring (D. Liu, Cui, Shang, & Zhong, 2021) and liquefied banana pseudo-stem in carrageenan/poly(vinyl alcohol) as a degradable copolymer film (Meng et al., 2018). To the best of our knowledge, no research work has reported on the combination of anthocyanin from *Ruellia squarrosa* (Fenzi) Cufod. flower with *κ*-carrageenan and poly(vinyl alcohol) for the development of smart film for freshness monitoring of food.

The aim of this study was to develop a smart packaging film of carrageenan and poly(vinyl alcohol) loaded with anthocyanin, a natural pH indicator, extracted

from *Ruellia squarrosa* (Fenzi) Cufod. flower using a solution casting and a sol-gel process. The fabricated smart films were characterized by scanning electron microscopy (SEM), Fourier transform infrared spectroscopy (FT-IR). The effects of film compositions on water vapor transmission rate (WVTR), antioxidant activity, UV protection, thermal stability, mechanical properties, biodegradability, pH-responsive color changes and their application as freshness indicator were also be studied.

1.2 Objectives

1. To develop the smart polymeric films composing κ-carrageenan/poly(vinyl alcohol) and nature extract obtained from *Ruellia squarrosa* (Fenzi) Cufod. flower for food freshness monitoring.
2. To evaluate the physicochemical properties and the responsive efficiency of the films in acid-base conditions and food spoilage responsiveness.

1.3 Scope of study

1. Preparation of polymeric film based on κ-carrageenan and poly(vinyl alcohol) containing natural extract from *Ruellia squarrosa* (Fenzi) Cufod. flower through a sol-gel reaction and a solution casting method.
2. Investigation on the physicochemical properties and biodegradability of the hybrid polymeric films by ATR-FTIR spectroscopy, SEM spectroscopy, UV-visible spectroscopy, thermal analysis, mechanical testing.
3. Evaluation of pH-responsive character of *κ*-carrageenan/poly(vinyl alcohol) film enriched with natural extracts from *Ruellia squarrosa* (Fenzi) Cufod. flower.
4. Application of the obtained smart films for spoilage monitoring of fresh food sample.

CHAPTER 2
LITERATURE REVIEWS

2.1 Smart packaging

Food packaging is utilized to protect the foods in the product from environmental condition such as heat, light, and microorganisms. The main functions of a package are containment, storage, delivery, protection, and communication on nutritional content of food (Schaefer & Cheung, 2018). It also plays important role in providing convenience and time saving for consumer. Nowadays, development of smart food packaging has been receiving increasing attention in the fields of food protection, quality monitoring, shelf-life extending and enhancing the safety of packaged products. Special functional compounds such as pH colorimetric indicators, antioxidants and antimicrobial agents have been incorporated in the smart packaging (Otles & Yalcin, 2008). Functional packaging systems can be divided into active and intelligent packaging. Concepts are depending on the useful interaction between packaging and the food in product. Active packaging is a new technology concept that can be designed to extend the shelf-life and to improve the quality of the food. This includes antimicrobial packaging, antioxidant packaging and moisture absorber (Biji, Ravishankar, Mohan, & Srinivasa Gopal, 2015). Intelligent packaging is created to communicate and deliver the information of the food in package to consumer that help in decision making based on food safety and quality (Otles & Yalcin, 2008). These active and intelligent packaging systems are essential in enhancement of quality, safety, and shelf-life of food products.

2.2 Natural extract

Ruellia squarrosa (Fenzi) Cufod. flower, generally called mexican petunia, can be used as a natural indicator due to its abundant anthocyanins which are high-quality pigments. It is well known that, the anthocyanin extracted from natural sources is a pH-responsive component in which its color change depends on the acid-base condition of the surrounding (Figure 2-1). A study reported on anthocyanins extracted from *Ruellia squarrosa* (Fenzi) Cufod. flower as an indicator for

development of a microfluidic paper–based analytical device with an obvious color change for the naked (Supalert, 2021). This natural extract could be an alternative for potential application in freshness indicator of food products.

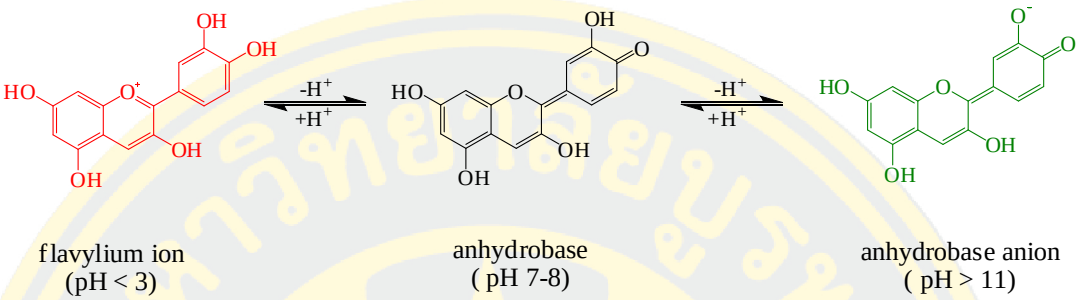

Figure 2-1 Structure of anthocyanins at difference pH conditions (Supalert, 2021).

2.3 Carrageenan

Biopolymeric carrageenan is an anionic sulfonated polysaccharide extracted from red edible seaweeds in the class Rhodophyceae. Its molecular structure composes of repeating disaccharidae unit with hydrophilic linear sulphated backbone of alternating D-galactose and 3,6-anhydrogalactose by α–1,3 and β-1,4 glycosidic linkages. There are three types of carrageenan, *κ*-carrageenan, *ι*-carrageenan, and *λ*-carrageenan depending upon the proportion and position of charged sulphate groups (Figure 2-2) (Y. Liu et al., 2019; Sedayu, Cran, & Bigger, 2019). *λ*-carrageenan consists of three sulfate groups in the molecular structure. This *λ*-carrageenan is generally used as thickener because it is easily soluble in solutions (Dille, Knutsen, & Draget, 2022). *ι*-carrageenan, a linear polysaccharide, composes two sulfate groups in molecular structure. This polymer has gel-forming characteristic and can be used as soft and flexible gel and film-forming material (Praseptiangga, Mufida, Panatarani, & Joni, 2021; Shen & Kuo, 2017). *κ*-carrageenan with one sulfate group in its repeating unit is made up of alternating 3-linked β-d-galactose 4 sulfate and 4 linked 3,6-anhydro α-d-galactose (J. Liu et al., 2018). Among the three types, *κ*-carrageenan has strong ability to form gels, good oxygen barrier and high solubility in hot water. Furthermore, *κ*-carrageenan has been extensively used for food packaging films due to the non-toxicity and film forming properties (Zakaria, Kamarudin, Kudus, & Wahid, 2022). On the other hand, *κ*-carrageenan film is generally known to have

limitations in the aspect of low mechanical and water resistance because of its high hydrophilicity. A number of studies have been carried out to enhance the properties of *κ*-carrageenan films. Preparation of polymeric blend has been successfully used to fabricate *κ*-carrageenan based film with high mechanical strength and thermal properties (Zakaria et al., 2022). *κ*-carrageenan film incorporated with curcumin has been reported to exhibit good oxygen and moisture barrier with high tensile strength (J. Liu et al., 2018).

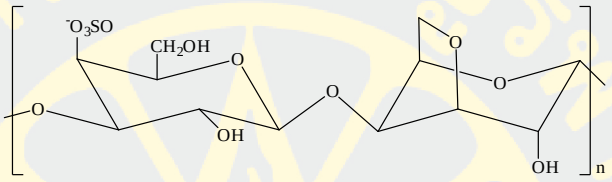

a) *κ*-carrageenan

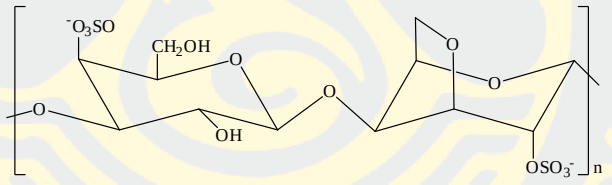

b) *ι*-carrageenan

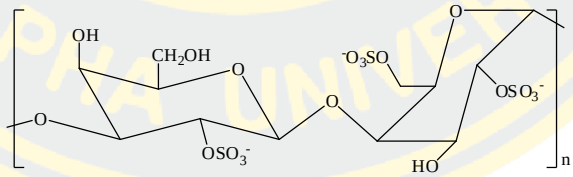

c) *λ*-carrageenan

Figure 2-2 Structure of different types of carrageenan (BeMiller, 2019)

2.4 Poly(vinyl alcohol)

Poly(vinyl alcohol) is a synthetic water soluble polymer and made up of hydrocarbon backbone. This polymer is manufactured by hydrolysis of polyvinyl acetate as its vinyl alcohol monomer is unstable. The acetate group of vinyl acetate can be hydrolyzed with methanol in the aqueous sodium hydroxide (Figure 2-3). The structure and physical characteristic of poly(vinyl alcohol) depend on the degree of

hydrolysis and the molecular mass. Poly(vinyl alcohol) is divided into two classes namely: fully hydrolyzed and partially hydrolyzed (Figure 2-4). Both types have been utilized for the food packaging materials (Muppalaneni, 2013; Nagarkar, 2019).

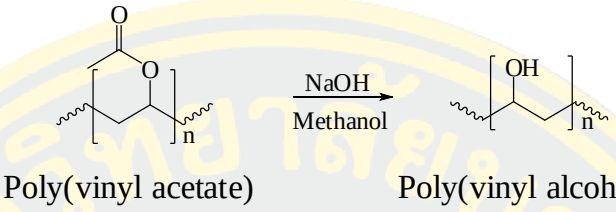

Figure 2-3 Synthesis of poly(vinyl alcohol)

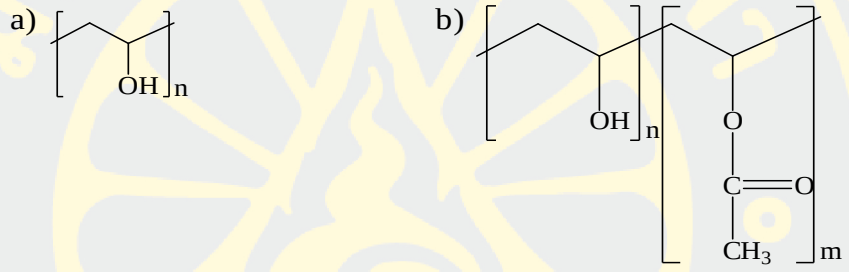

Figure 2-4 Structural formula for poly(vinyl alcohol): a) fully hydrolyzed, b) partially hydrolyzed (Mok et al., 2020)

Generally, poly(vinyl alcohol) is whitish powdered with characteristics of film forming, high viscosity, hydrophilic nature, harmless and nontoxicity (Aslam, Kalyar, & Raza, 2018; Ben Halima, 2016). It has been widely used for several applications such as biomedical scaffold, fiber, coating, and packaging due to its flexibility, transparency, non-toxicity, and high mechanical properties (B. Liu, Zhang, & Guo, 2022). Studies on the incorporation of poly(vinyl alcohol) into biopolymers such as chitosan, carboxymethyl cellulose and gelatin have shown enhancement in mechanical and physical properties of the films (Kanatt, Rao, Chawla, & Sharma, 2012).

2.5 Sol-gel process

A sol-gel process has been generally investigated and used for modification of polymers. The process can be started from reactions of inorganic polymerization with a wide variety of inorganic and alkoxide precursors. In the transition process, a sol is

a dispersion of colloid particles within a liquid in which colloid particles have diameters of 1-1000 nm. A gel can be interconnected porous solid network yielding macromolecules of polymeric chains (Pierre, 2020). The sol-gel has been widely utilized to fabricate thin films and powder catalysts (such as chemical sensors, fibers, membranes, and photochromic applications) (Akpan & Hameed, 2010). The sol-gel reaction proceeds through and condensation of water and alcohol follows:

Hydrolysis:	M-O-R + H_2O	→	M-OH + R-OH
Water Condensation:	M-OH + HO-M	→	M-O-M + H_2O
Alcohol Condensation:	M-O-R + HO-M	→	M-O-M + R-OH

When M represents a metal (Zr, Si, Sn, Al and Ti) and OR represents alkoxy (Trakulsujaritchok & Suksai, 2018).

Hydrolysis of metal alkoxide precursors such as tetraethoxysilane (TEOS), can be simply reacted by adding water into metal alkoxides (Figure 2-5).

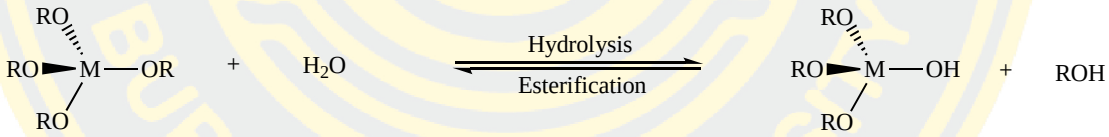

Figure 2-5 Hydrolysis of metal alkoxides.

Condensation is continued by linking the hydrolyzed molecules together. During this step, a polymer network structure is formed and small molecules such as water or alcohol are liberated (Figure 2-6) (Ismail, 2016).

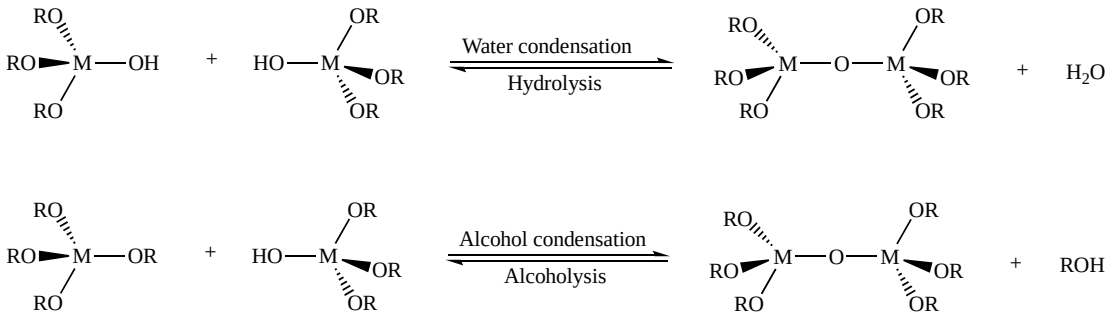

Figure 2-6 Condensation of hydrolyzed molecules.

2.6 Characterization techniques

2.6.1 Attenuated total reflectance Fourier transform infrared spectroscopy (ATR-FTIR)

Attenuated total reflectance Fourier transform infrared spectroscopy is one of the spectroscopic techniques well-known for identification of specific functional groups in sample. Samples can be analyzed using ATR-FTIR as solids, liquids, suspensions, and thin films. The absorption process of photon in the infrared radiation of frequency occurs when the molecule is stimulated to a higher vibrational state. In ATR spectroscopy, a crystal is utilized for total reflection. The sample is put on crystal and then the IR Beam is directed through the crystal and totally internally reflected at the interface of infrared transparent material with high refractive index. Total reflection process can pass through of sample in a few micrometers and a part of radiation is absorbed into sample (Figure 2-7) (Chianese, Angelo, J, Kramer, & eds, 2012; Santos, Morais, & Lima, 2021).

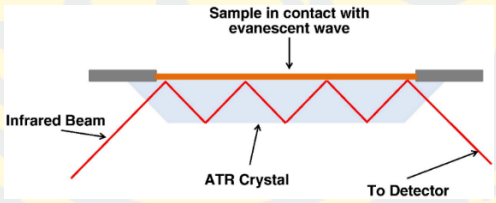

Figure 2-7 The reflection of infrared beam of ATR-FTIR spectroscopy (Shai, 2013)

2.6.2 Ultraviolet-Visible (UV-VIS) Spectroscopy

Ultraviolet-visible spectroscopy can be used as an analytical technique, although unknown compound identification could not present by this alone technique. The technique has been carried out on certain tasks with potential efficiency. The principle is based on the absorption of UV-light by a molecule, resulting in a spectrum of absorbance and wavelength. Ultraviolet-visible spectroscopy can be used in rapid analysis with high accuracy and simple experiment (Campbell, Pethrick, & White, 2000).

2.6.3 Thermogravimetric analysis (TGA)

Thermogravimetric analysis, a technique of weight measurement, is used for evaluation of the mass of a specimen as a function of temperature or time. During the analysis, a specimen is under investigated temperature range and atmosphere. The specimen is commonly heated with a constant heating rate (dynamic method) or kept with a constant temperature (isothermal method). The temperature ranges for analysis are generally higher than 500 °C or more and the atmosphere can be inert gas such as nitrogen, argon, or helium. The result of thermogravimetric analysis is demonstrated in the TGA curve while percent of mass or mass formed against time or temperature is shown in DTG thermogram (Bottom, 2008; Menczel & Prime, 2009).

2.6.4 Colorimetric Analysis

Color, an optical property, indicates first characteristic of products and plays a role of importance for decision of the consumer. The CIELAB system is used for color value measurement with the results presented in terms of L*, a* and b* parameters using the concept of trichromatic principle. The system composed of the three-dimensional space defined by L*, a*, and b*(Figure 2-8), where:

L* parameter defines lightness on a scale that varies from black (0) to white (100).

a* parameter defines from green (-) to red (+).

b* parameter defines from blue (-) to yellow (+).

In addition, color differences (ΔE) between two color values of CIELAB space are calculated from Euclidean distance during their place in the three-dimensional space by applying mathematic following equation:

$$\Delta E = \sqrt{(\Delta L)^2+(\Delta a)^2+(\Delta b)^2}$$

where ΔL, Δa and Δb are expressed the difference of lightness and each color values (de Matos et al., 2021; Macdougall, 2010).

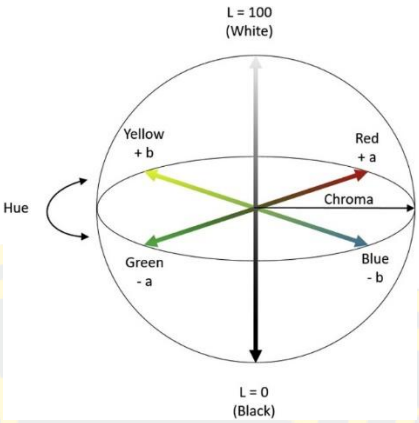

Figure 2-8 The diagram of CIELAB color system (Ly, Dyer, Feig, Chien, & Del Bino, 2020).

2.6.5 Tensile testing

Tensile testing is a method generally used for evaluation of mechanical properties for applications. Tensile testing involves deformation of specimen using tensile force under controlled condition until breaking of specimen (Figure 2-9). The test presents information about tensile strength, tensile modulus, elongation, and percent of elongation at break that can be calculated as follows (Davis, 2004; JOSE MATHEW & Francis, 2020):

$$\text{Tensile strength (MPa)} = F/A$$

where F is the force to elongate the specimen (N).

A is the cross-sectional area of the specimen (m^2).

$$\text{Elongation (\%)} = (\Delta L/L_0) \times 100$$

where ΔL is the difference in length of the specimen under applied force.

A is the cross-sectional area of specimen.

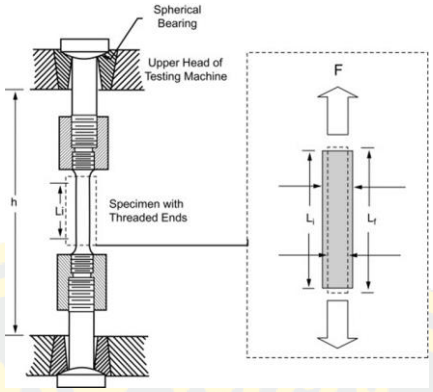

Figure 2-9 The diagram of typical tensile testing (Farhat, 2021).

2.6.6 Scanning Electron Microscopy (SEM)

SEM is an electron microscopy technique widely used in many fields of polymer analysis such as membrane surface and cross-sectional morphology due to its high efficiency resolution. SEM composed of electron gun as a source of generated electrons with high energy in ranging around 100-30,000 electron volts or more (Figure 2-10). The electron beam is focused by condenser lenses as beam with a focal spot of size 1 -5 nm upon the specimen to create the signals used to produce the image called micrograph. The micrograph is produced by moving of the scan coils depending on the magnification required. Then, the scattering of emitted electron beam (signals) is detected by electron detector to produce an image (Balaji Ganesh & Radhakrishnan, 2006; Mohammed & Abdullah, 2018).

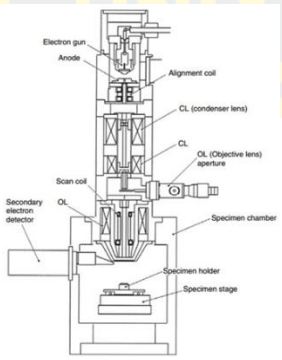

Figure 2-10 Components of a scanning electron microscope (Tursunov et al., 2015).

2.7 Literature reviews

J. Liu et al., 2018 developed *κ*-carrageenan based film containing curcumin for monitoring of pork and shrimp freshness. The fabricated films were investigated for their thermal stability, barrier properties, tensile strength, microstructure, and pH change sensing. The results indicated that incorporation of curcumin could improve the barrier and tensile properties and enhance of thermal stability of the films. In addition, the film exhibited change of color in different pH conditions that could be noticed as a redness-shift in color under alkaline. Then, the developed *κ*-carrageenan/curcumin films were applied as spoilage indicator of samples during storage. Color of the films changed from yellow to red on the third day of freshness monitoring (Figure 2-11). Development of the film composed *κ*-carrageenan and curcumin showed strong potential for monitoring of pork and shrimp in foods industry.

Figure 2-11 κ-carrageenan/curcumin films for freshness monitoring of pork and shrimp (J. Liu et al., 2018).

Yong et al., 2019 prepared chitosan films incorporated with anthocyanin from purple sweet potato extract (PSPE) for development of intelligent pH-sensing films. Investigation on the antioxidant, pH-sensitive and physical properties of developed films showed that addition of anthocyanin could improve the physical properties such as UV–vis light barrier property, thermal stability, antioxidant potential and pH-sensing ability of the films. However, the samples incorporated with anthocyanin exhibited lower crystalline character, elongation at break and moisture content due to interrupted chain-chain interactions in chitosan structure. The chitosan-PSPE films could respond to pH with color changing from pink-red (pH 3.0–6.0) to purple-brown

(pH 7.0–8.0) to final greenish–green (pH 9.0–10.0) (Figure 2-12). Antioxidant ability of chitosan-PSPE films was found to increase with increasing PSPE extracts. The pH-sensing ability of prepared films was investigated and proofed to be potential for the application of food spoilage monitoring (with fresh fish and pork samples) and food packaging with antioxidant abilities.

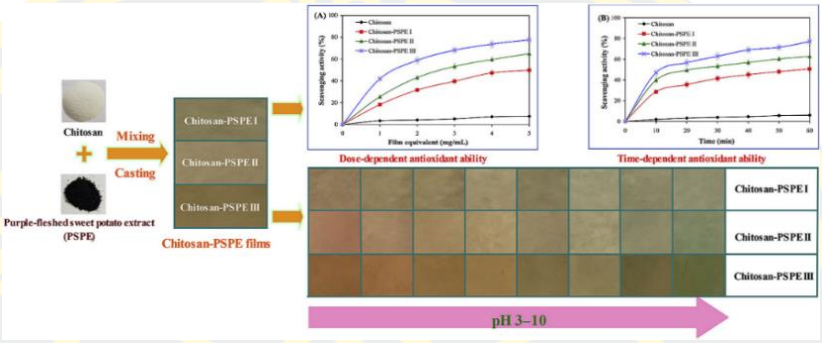

Figure 2-12 Chitosan-PSPE films for the application of pH-sensitive and antioxidant ability (Yong et al., 2019).

Peralta, Bitencounrt-Cervi, Maciel, Yoshida, & Carvalho, 2019 developed an intelligent packaging system derived from natural polymers (starch, gelatin, and chitosan) composing of anthocyanin as a pigment obtained from aqueous hibiscus extract (HAE). Films of difference natural polymers incorporated with HAE were prepared by solution casting and evaluated for their water content, total soluble matter, scanning electronic microscopy and color change at different pH values as a rapid pH indicator. The fabricated starch and gelatin films showed pink color whereas the chitosan base film was light brown due to the different of chelation forms in the films. Addition of aqueous hibiscus extract enhanced the moisture content of the films and increased total soluble matter values especially in starch films containing HEA. The effect of pH values to color change was investigated and reported that starch and gelatin films at pH 2-4 displayed red color, brown to lightly greenish color at pH 5-8 and yellow color at pH 13.0. The chitosan containing HAE film showed less pronounced differentiation of color change with pH (Figure 2-13). Consequently, development of aqueous hibiscus extract combined natural polymeric films (starch,

gelatin, and chitosan) could offer a choice of pH indicators in packaging for safety and quality of packed foods.

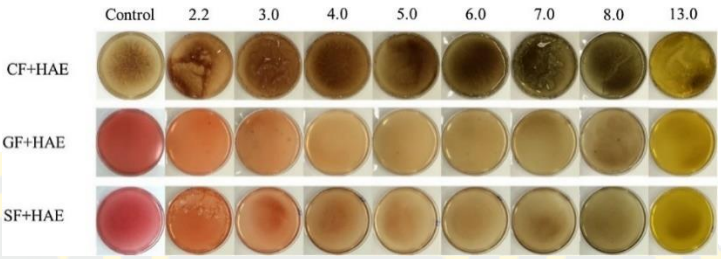

Figure 2-13 Color changes of the hibiscus extract incorporated films at different pH conditions (Peralta, Bitencourt-Cervi, Maciel, Yoshida, & Carvalho, 2019).

Singh, Nwabor, Syukri, & Voravuthikunchai, 2021 investigated biodegradable films obtained from chitosan and polyvinyl alcohol (CHP) with an addition of anthocyanins from *Clitoria ternatea* (CT) flower and *Carissa carandas* (CC) fruit by solvent casting method. Colors of CHP–CT and CHP-CC films were light green and brownish, respectively. The developed copolymer films were evaluated for their mechanical, and physical properties, and colorimetric sensitivity for freshness monitoring of pasteurized orange juice and cow milk. The results showed that the addition of extracts resulted in increased WVP, whereas the water solubility, swelling index, tensile strength and Young's modulus were decreased. Furthermore, the color change response of the prepared films for beverage freshness demonstrated that the color of CHP–CC films tested with juice at 25 °C for 72 h changed from yellowish-green to brownish yellow, depending on the extract content (Figure 2-14). The resulted of photo-degradation of anthocyanin within films revealed that these films possessed stability when stored in dark at 4 °C and 25 °C. Consequently, the films containing anthocyanins exhibited suitable pH sensing property which could be applied for indicator of beverages freshness.

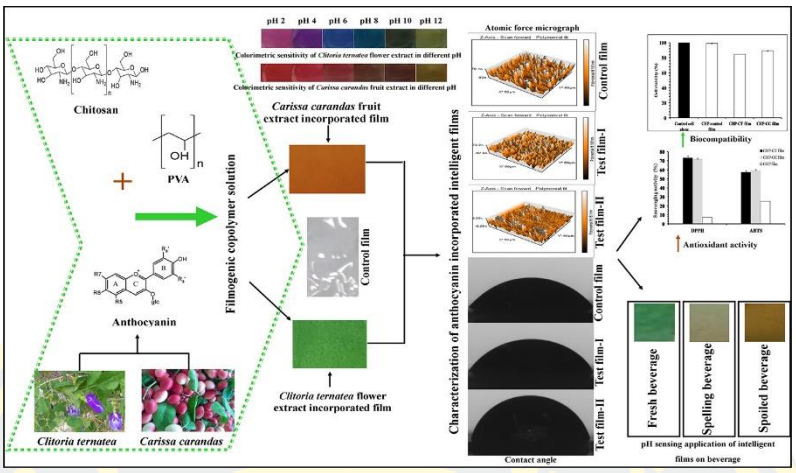

Figure 2-14 Anthocyanin-rich chitosan/poly(vinyl alcohol) films: production and their properties (Singh, Nwabor, Syukri, & Voravuthikunchai, 2021).

Sobhan, Muthukumarappan & Wei, 2022 fabricated biodegradable films based on cellulose-nanofiber/chitosan dyed with methyl red (CCM) and single layer coated with polylactic (PLA) for the application of food spoilage monitoring. The PLA/CCM films were investigated in terms of morphology, anti-microbial activity, thermal and barrier properties. These films were studied for indicator ability of beef and fish spoilage at room temperature (23 °C). The films exhibited enhanced properties in thermal stability and lower in water vapor transmission rate. The developed films responded to different pH conditions by displaying color change from red to yellow after 1 day. Changes of PLA/CCM films were measured with beef and fish spoilage and found that the color changed from red to yellow after 1 day. In addition, the biodegradation of PLA/CCM films revealed effectively increase percentage of weight loss after 1-5 week with cracking down of films.

Akhila, Sultana, Ramakanth, & Gaikwad, 2023 prepared poultry packaging films by incorporating *Ipomoea coccinea* extract (ICE) into polyvinyl alcohol (PVA)/guar gum (GG) blend and used for monitoring the freshness of chicken. The developed film was characterized through thermogravimetry, water solubility, water contact angle, and surface morphology. Additionally, the pH indicator potential was examined in terms of color responsiveness to various pH conditions and freshness monitoring of chicken fillets. The resulting film containing ICE demonstrated a

decrease in mechanical properties with an increase in ICE concentration. However, the incorporation of ICE improved water vapor transmission rate and crystallinity of the film, as well as imparted strong antioxidant activity. The fabricated film displayed a color change to red at pH 2 and to yellowish-green at pH 13. The results confirmed that the fabricated packaging exhibited potential application as a pH indicator for monitoring the freshness of chicken.

Figure 2-15 Preparation and application of poly(vinyl alcohol)/guar gum film containing Ipomoea coccinea extract for an intelligent pH indicator (Akhila, Sultana, Ramakanth, & Gaikwad, 2023).

Goudarzi, Moshtaghi, & Shahbazi, 2023 produced electrospun fiber mats based on κ-carrageenan-poly(vinyl alcohol) combined with *Prunus domestica* extract (PDE) and epigallocatechin gallate (EGCG) for the application of intelligent packaging materials. The tensile strength, water vapor permeability, moisture content, and water solubility of the anthocyanin-rich electrospun fibers were characterized. Their antimicrobial and antioxidant activities were also examined. The prepared electrospun fibers containing PDE and EGCG exhibited good fiber forming ability and homogeneity. They displayed a color change from light pink to brown in response to changes from acidic to basic conditions. After the incorporation of PDE and EGCG, the electrospun fibers demonstrated improved thermal stability, moisture resistance, and water solubility. In addition, they exhibited increased thickness and elongation at the break point. The fiber mats responded to the presence of ammonia

gas with color changes from white to brown. They also responded to changes in the pH of beef meat during refrigerated storage with color changes from white to purplish-red from day 0 to day 15.

Khan, Riahi, Kim, & Rhim, 2023 fabricated the gelatin/carrageenan films by incorporating Cu-metal organic framework (Cu-MOF) and anthocyanin extracted from red cabbage for the real-time freshness monitoring of shrimp. The UV-light barrier, antimicrobial, antioxidant activity, and pH-responsive properties of the films were characterized. The prepared films exhibited rough surfaces and clusters of particles with good compatibility within the matrix. Their antibacterial, antioxidant and mechanical properties were improved after addition of Cu-MOF and anthocyanin. The composite films exhibited excellent UV-blocking properties, making them suitable for the application in packaging of UV-sensitive food. The films containing Cu-MOF and anthocyanin exhibited color changes from reddish to greenish-yellow in response to pH conditions, indicating the spoilage of shrimp during storage at 28 °C for 24 h. Therefore, the films based on gelatin/carrageenan containing Cu-MOF and anthocyanin could potentially be used for active and smart food packaging.

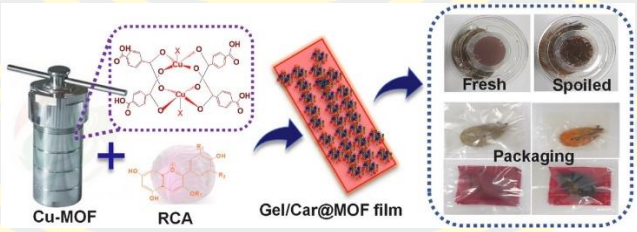

Figure 2-16 Gelatin/carrageenan containing Cu-MOF and anthocyanin for active and smart packaging film (Khan, Riahi, Kim, & Rhim, 2023).

Miao et al., 2023 fabricated smart films from riclin and poly(vinyl alcohol) for food freshness monitoring using anthocyanin based on purple sweet potato as a pH indicator. The mechanical and barrier biodegradability and antioxidant properties of prepared films were studies. The physical properties of the developed films were improved with enhancing the mechanical and barrier properties through hydrogen bonding between riclin and poly(vinyl alcohol). The films demonstrated

biodegradability and antioxidant activity after incorporating riclin into poly(vinyl alcohol). Additionally, the indicator function of the films was examined using shrimp and demonstrated high efficiency with color changes from violet-red to yellow-green within 24 h. Therefore, the biodegradable composite films could potentially be used for monitoring food freshness with high sensitivity to pH conditions and ammonia gas.

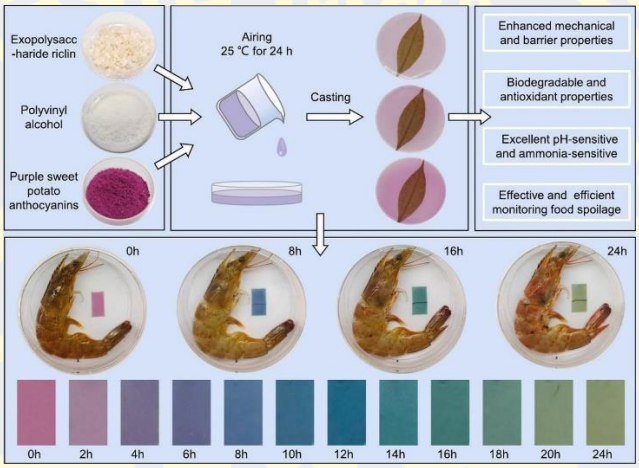

Figure 2-17 Biodegradable composite films of riclin/poly(vinyl alcohol) incorporated with purple sweet potato anthocyanins: preparation and application of food freshness monitoring (Miao et al., 2023).

Li, Wang, Fang, Zhuang, & Zhu, 2024 prepared a smart film of chitosan/gelatin incorporating with anthocyanin extracted from butterfly pea flowers (BAE) that responded to the volatile amines for food freshness indicator. The physical properties of the prepared film were characterized, including its morphology, mechanical property, and water vapor permeability. In addition, the indicator part of the anthocyanin-contained film was examined in terms of color stability, antioxidant activity, and color responsiveness. The film exhibited a homogeneous surface after the incorporation of BAE. The inclusion of BAE in the metrics resulted in an increase in thickness, flexibility, and elasticity. Additionally, the prepared film exhibited good antioxidant properties and color stability. In response to pH values, the film containing BAE displayed a transition from light pink to blue-purple within the pH range of 2-7, and under alkaline conditions, the color of the film turned green. The

developed film demonstrated good amine sensitivity and could be used to detect beef freshness through color changes that indicated food spoilage.

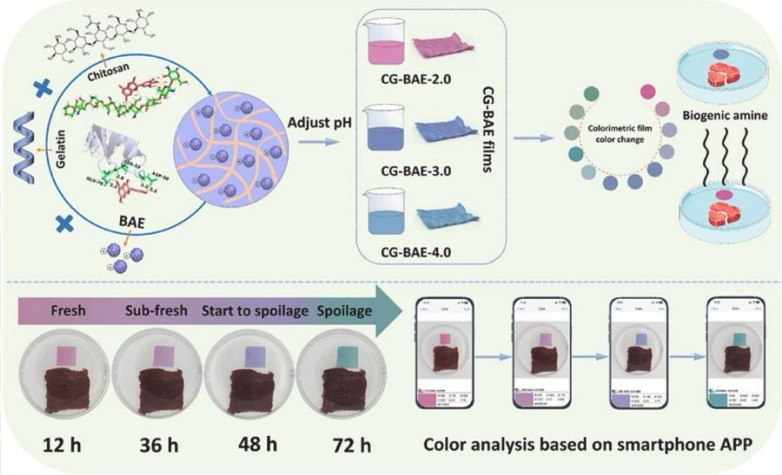

Figure 2-18 Preparation and application of chitosan/gelatin film and anthocyanin for beef sub-freshness monitoring (Li, Wang, Feng, Zhuang, & Zhu, 2024).

L. Li et al., 2024 developed multifunctional films based on gallic acid-modified chitosan (GCS) and gelatin through a polyelectrolyte complex. The developed films were incorporated with garlic essential oil emulsion and crude anthocyanin extracted from garlic and purple cabbage. Properties of the films were investigated including mechanical strength, barrier capacity, antibacterial and antioxidant activities. The results showed that tensile property, antioxidant and antibacterial activities were improved after incorporation of gallic acid-modified chitosan and garlic essential oil emulsion with gelatin. Additionally, the prepared films containing anthocyanins exhibited pH-responsive properties with color changes from light red to yellow-green under pH 1-13 conditions, indicating potential material for monitoring fish freshness. The smart labels were tested by wrapping of fish at 4 °C for 3 days and it was found that color of the films changed from dark brown to gray according to freshness of the fish.

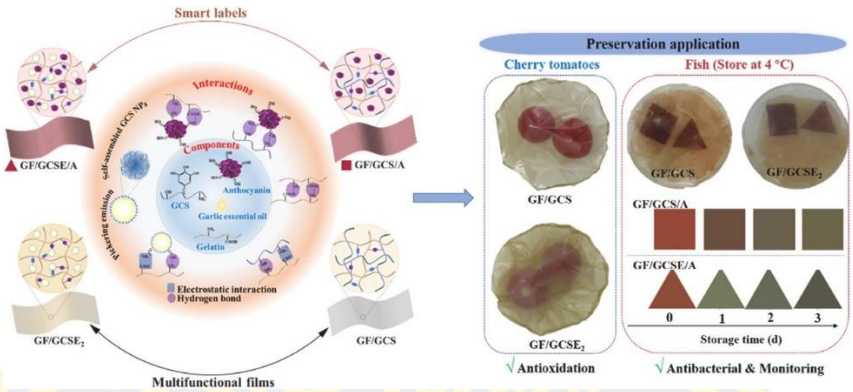

Figure 2-19 Multifunctional films based on gallic acid-modified chitosan (GCS) and gelatin as smart labels for monitoring the freshness of fish and preserving cherry tomatoes (L. Li et al., 2024).

CHAPTER 3
RESEARCH METHODOLOGY

3.1 Materials

1. κ-Carrageenan, CAS Number 11114-20-8 (Tokyo Chemical Industry)
2. Poly(vinyl alcohol), MW. 60000 g/mol, degree of hydrolysis 98%, CAS Number 9002 89-5 (Merck)
3. *Ruellia squarrosa (Fenzi)* Cufod. flower extract
4. Tetraethyl orthosilicate, CAS Number 78-10-4 (Acros Organics)
5. Gallic acid monohydrate, CAS Number 5995-86-8 (Fluka)
6. Folin Ciocalteu's reagent, CAS Number 463562 (Carlo Erba)
7. Sodium carbonate anhydrous, CAS Number AF405220 (Ajax Finechem)
8. Ferric chloride hexahydrate, CAS Number 10026-77-1 (Quality Reagent Chemical)
9. 2,2-Diphenyl-1-picrylhydrazyl, CAS Number 1898-66-4 (Aldrich Chemistry)
10. Sodium acetate anhydrous, CAS Number 127-09-3 (Leonid Chemicals)
11. Dimethyl sulfoxide, CAS Number 67-68-5 (RCI Labscan Limited)
12. Ammonium hydroxide, CAS Number 90-090 (Gammaco)
13. Potassium chloride, CAS Number 1411181937 (Ajax Finechem)
14. Methanol, CAS Number 67-56-1 (Loba Chemie)
15. Sodium hydroxide, CAS Number 1310-73-2 (Merck)
16. Hydrochloric acid, CAS Number 7647-01-0 (Quality Reagent Chemical)
17. Ethanol, 99.9% Grade AR (Quality Reagent Chemical)
18. Ethanol, 95% Commercial grade (CT chemical)

3.2 Instruments

1. Attenuated total reflectance Fourier transform infrared spectrometer (ATR-FTIR), model Frontier, PerkinElmer
2. Texture analyzer, model TA.XTplus, Stable micro systems
3. Scanning electron microscope-energy dispersive X-ray spectrophotometer (SEM-EDX), model LEO 1450 VP, Carl ziess

4. Double beam UV-VIS spectrophotometer, model UV-2600, Shimadzu
5. Microplate reader spectrophotometer, model EPOCH-2, BioTek
6. UV-Visible Spectrophotometer, model Cary 3500, Agilent
7. Colorimeter, model WR-10, Shenzhen Wave Optoelectronics Technology
8. Thermogravimetric analyzer, model Pyris 1, Perkin Elmer
9. Rotary evaporator, model Rotavapor R-3, Buchi

3.3 Preparation of *Ruellia squarrosa (Fenzi)* Cufod. crude extract (R)

1. Fresh *Ruellia squarrosa (Fenzi)* Cufod. flowers were collected and shredded using a blender. Extraction was done by immersing the shredded flower in 70% ethanol at a flower-solvent ratio of 1:10 for 24 h. The extract solution was filtered through a funnel containing cotton. The remaining solid was repeatedly extracted two times by the same method.

2. The organic solvent was evaporated from the extract solution using a vacuum rotary evaporator at 50 °C. The obtained crude extract (R) was kept at 4 °C until used.

3.4 Characterization of the crude extract

3.4.1 pH-responsive character

The colorimetric change of the crude extract solution obtained from *Ruellia squarrosa* (Fenzi) Cufod. flowers was examined under different pH values ranging from 1 to 12. 250 µL of the extract solution (0.16% w/v) in distilled water was added in a vial containing 6 mL of each pH solution (pH 1-12). After that, the mixed solutions were analyzed by a UV-2600 spectrophotometer. The absorbance spectra in wavelength range of 200 to 800 nm were reported.

3.4.2 Evaluation of antioxidant activity using DPPH assay

Antioxidant capacity of the *Ruellia squarrosa* (Fenzi) Cufod. crude extract was determined using 2,2-diohenyl-1-1picrylhydrazyl (DPPH) radical scavenging assay. For this analysis, 1 mL solution (50 mg/mL) of crude extract in 99.9% ethanol was prepared and used as a stock solution to obtain 1.25, 0.63, 0.31, 0.16 mg/mL

solutions. 20 µL of each crude extract solution was transferred to a microplate well and mixed with 180 µL of 0.24 mM DPPH in ethanol solution. Thereafter, these samples were incubated in the dark for 30 min at room temperature. The absorbance was measured at wavelength 517 nm using a microplate reader spectrophotometer (Bio Tek Instruments). The DPPH inhibition value was calculated using following equation (Athipornchai, Kumpang, & Semsri, 2021):

$$\text{DPPH inhibition (\%)} = \frac{A_{DPPH} - A_{extract}}{A_{DPPH}} \times 100$$

where A_{DPPH} is the absorbance of DPPH solution of a control (composed of all reagents except the extract sample) and $A_{extract}$ is the absorbance of the extract mixed solution.

3.4.3 Total phenolic and Total *ortho*-hydroxyphenolic content

Total phenolic content (TPC) of the crude extract was evaluated using the Folin-Ciocalteu's reagent and the standard curve was established using gallic acid (GA). Briefly, 50 mg of the extract sample was dissolved in 1 mL of DMSO. The obtained sample (20 µL) was then mixed with 100 µL of 10% v/v Folin-Ciocalteu's reagent in a 96-well plate and incubated for 5 min in the dark. Then, 80 µL of 2.5% w/v Na_2CO_3 solution was added and kept for 30 min in the dark at room temperature. The absorbance was measured at wavelength 760 nm using a microplate reader spectrophotometer (Bio Tek Instruments). The TPC was reported as mg of gallic acid equivalents/g extract (mg GAE/g extract) (Athipornchai & Jullapo, 2018).

Total *ortho*-hydroxyphenolic content (TOHPC) of the crude extracts was measured according to the method reported by Athipornchai & Klangmanee, 2021. For this analysis, 50 mg of the crude sample was dissolved in 1 mL of DMSO. 100 µL of the obtained solution was transferred to a 96-well plate and mixed with 100 µL of 1% w/v $FeCl_3$ methanolic solution. Then, the solution was incubated in the dark for 30 min at room temperature. The solution absorbance was measured at wavelength 695 nm using a microplate reader spectrophotometer. The TOHPC was reported as mg of gallic acid equivalents/g extract (mg GAE/g extract).

3.4.4 Total anthocyanin content

The pH differential assay was used to determine total anthocyanin content (TAC) of the crude extract (Inacio, de Lima, Lopes, Pessoa, & de Almeida Teixeira, 2013; Moradi, Tajik, Almasi, Forough, & Ezati, 2019). 50 mg of the crude extract was dissolved in 1 mL of DMSO. The obtained extract sample (10 µL) was added with 90 µL of 0.025 M potassium chloride solution in a well plate. In another well, the extract sample (10 µL) was added with 90 µL of 0.4 M sodium acetate solution. Then, each mixed solution was kept in the dark for 1 h and the absorbance was determined at wavelength 510 and 700 nm using a microplate reader spectrophotometer. The TAC was calculated as mg cyanidin-3-O-glucoside equivalent /100 g of dry weight extract solution by the following equation.

$$A = (A_{510} - A_{700})_{KCl} - (A_{510} - A_{700})_{NaOac}$$

$$\text{Total anthocyanin content (mg CAE /100 g DW)} = \frac{A}{\varepsilon \times \iota} \times MW \times DF \times \frac{V}{W} \times 100$$

where A is the absorbance value, ε is the molar extinction coefficient of cyanidin-3-O- glucoside (26,900 L/mol.cm), MW is the molecular weight of cyanidin-3-glucoside (449.2 g/mol), DF is dilution factor, V is the volume (mL) of solute used for preparing the extract solution and W is sample weight (mg).

3.5 Preparation of κ-carrageenan/poly(vinyl alcohol) films

1. 0.40 g of κ-carrageenan powder was dissolved in 10.0 mL of distilled water with constant stirring at 80 °C for 2 h.

2. 15.0 mL of poly(vinyl alcohol) solution (4% w/v) was added into the *κ*-carrageenan solution with continuous stirring at 80 °C for 2 h. After that, the temperature was brought down to 60 °C.

3. 1.0 mL of ethyl alcohol (99.9%) was added into the polymer blend solution with continuous stirring at 60 °C for another 30 min. Then, 45 µL of TEOS was added into the homogenized solution and kept stirring at 60 °C for 12 h. In the case of films incorporated with natural extract (R),the reaction time was optimize to 20 h.

4. Thereafter, a required amount of *Ruellia squarrosa* (Fenzi) Cufod. flowers crude extract was dissolved in distilled water (500 µL) and added to the solutions with stirring at 60 °C for 30 min.

5. The final solution was transferred into petri-dishes and dried at 60 °C for 20 h. The dried κ-carrageenan/poly(vinyl alcohol) films were kept in a desiccator at room temperature.

Table 3-1 Chemical compositions of κ-carrageenan/poly(vinyl alcohol) films composed of *Ruellia squarrosa* (Fenzi) Cufod flower extract (R).

Sample	KC (g)	DI water (mL)	4% PVOH (mL)	EtOH (mL)	TEOS (µL)	R[a] (g)
40KC/60PV	0.40	10.0	15.0	0	0	0
50KC/50PV	0.50	12.5	12.5	0	0	0
60KC/40PV	0.60	15.0	10.0	0	0	0
40KC/60PV-T45[b]	0.40	10.0	15.0	1.0	45.0	0
40KC/60PV-T45-0R	0.40	10.0	15.0	1.0	45.0	0
40KC/60PV-T45-5R	0.40	10.0	15.0	1.0	45.0	0.05
40KC/60PV-T45-10R	0.40	10.0	15.0	1.0	45.0	0.10
40KC/60PV-T45-20R	0.40	10.0	15.0	1.0	45.0	0.20
40KC/60PV-T45-30R	0.40	10.0	15.0	1.0	45.0	0.30

[a]: weight of the crude extract dissolved in 500 µL of DI water.

[b] the reaction time for 12 h

3.6 Characterization of films

3.6.1 Attenuated total reflectance Fourier transform infrared spectroscopy (ATR-FTIR)

Functional group analysis of *κ*-carrageenan/poly(vinyl alcohol) film samples were characterized using an ATR-FTIR spectrometer at a wavenumber range of 400-4000 cm^{-1} and a resolution of 4 cm^{-1}, with 4 scans per sample.

3.6.2 Scanning electron microscopy-energy dispersive X-ray (SEM-EDX)

The surface morphology and elemental composition of the film samples were characterized using a scanning electron microscope (LEO 1450 VP model Carl ziess) equipped with an energy dispersive X-ray spectrophotometer (EDX). The films were placed onto aluminum stubs with carbon tapes and coated with gold sputtering.

3.6.3 Mechanical properties

Tensile strength (TS) and percent elongation at break (%EB) of specimens were measured using a texture analyzer according to ASTM D882-91. Five specimens (1 cm × 5 cm) were cut from each film. The specimens were mounted with 30 mm grip distance and stretched at a crosshead speed of 1.0 mm/sec. The TS and %EB of the specimens were determined from the stress-strain curves and Young's modulus were calculated from the slope of the initial linear part.

3.6.4 Percentage of moisture content

The film samples (2cm × 2cm) were dried to constant weights in a hot air oven at 110 °C for 10 min, cooled down in a desiccator and weighed (W_O). The films were left in room conditions for 24 h and weighed (W_F). Moisture content in the film samples was determined by calculating the difference in weights before and after moisture adsorption of the films using the following equation:

$$\text{Moisture content (\%)} = [(W_F - W_O)/W_O] \times 100$$

where W_O and W_F were the sample weights before and after moisture adsorption test, respectively.

3.6.5 Swelling ratios and solubility

The films (2cm × 2cm) were weighed and immersed in 30 mL of deionized water. At certain time intervals, the swollen films were taken out of the medium and reweighed. Swelling ratio of the films was calculated using the following equation:

$$\text{Swelling ratio (g/g)} = (W_F - W_O)/W_O$$

where W_O and W_F were the sample weights before and after swelling test, respectively.

After swelling test, the swollen films were taken out of deionized water, oven dried (110 °C, 2 h) and weighed (W_S). %Solubility was calculated using the following equation:

$$\text{Solubility (\%)} = [(W_O\text{-}W_S)W_O] \times 100$$

where W_O and W_S were the sample weights before and after swelling test, respectively.

3.6.6 Water vapor transmission rate (WVTR)

Water vapor transmission rate (WVTR) was evaluated using the cup method. Briefly, 20 g of silica gel (0%RH) is added to a cup covered with the fabricated film. The cups were placed in a desiccator containing oversaturated solution of sodium chloride and then the weight of the cups was measured at periodically intervals of 5 days using an analytical balance. The WVTR of film was calculated from the slope of weight changes (ΔW) at specified durations (Δt) divided by the specific area of the films (A) using the following the equation (Forghani, Zeynali, Almasi, & Hamishehkar, 2022):

$$\text{Water vapor transmission rate } (g/m^2.h) = \frac{\Delta W}{\Delta t \times A}$$

3.6.7 Light barrier property

The light barrier property of the films was measured using a UV-2600 spectrophotometer (Shimadzu). The transmittance of the films was measured in the range of 200 to 800 nm. For film transmittance testing, each film sample (3 cm × 5 cm) was placed in a film holder and then the transmittance of the sample was measured.

3.6.8 Thermal stability

The thermal stability of the films was analyzed by a thermogravimetric analyzer (TGA). For this, the film sample was weighed, placed into an aluminium pan and heated from room temperature to 700 °C at a heating rate of 10 °C/min under N_2 atmosphere.

3.6.9 Colorimetric analysis

The differences in color of the prepared film were measured with response to alkali gas using a WR-10 colorimeter (Shenzhen Wave Optoelectronics Technology), where the values of L (lightness), a (red/green), and b (yellow/blue) were recorded. The film samples were attached to the lid of the cup containing ammonia solution (1, 3 and 5%v/v). The samples being placed above the ammonia solution level at 1.5 cm were analyzed for their color changes at periodically from 2 min to 72 h (Wang et al, 2022). The value of color difference (ΔE) was be calculated by equation (J. Liu et al., 2018):

$$\Delta E = [(L^* - L)^2 + (a^* - a)^2 + (b^* - b)^2]^{0.5}$$

where L*, a* and b* are the initial values of lightness, redness, and yellowness, whereas L, a and b are the values after exposure to the test condition.

3.6.10 pH-sensitive ability

The pH-sensitivity of films as an indicator was evaluated by immersing the film sample (2 cm × 2 cm) in 10 mL of various pH solutions (pH 1-12) for 2 min. Then, the samples were taken out of the pH solutions and allowed to dry at room temperature for 5 min. The color changes of film samples were photographed using a digital camera and measured by a WR-10 colorimeter (Shenzhen Wave Optoelectronics Technology) (Zhang et al., 2019).

3.6.11 Biodegradation

The biodegradability of the film samples was evaluated by a modified method reported by Amaregouda and co-workers (Amaregouda, Kamanna, & Gasti, 2022).

Briefly, the film samples with the size of 3 cm × 3 cm were dried in a hot air oven at 80 °C for 10 min and weighed. After that, the weighed films were buried in soil at a depth of 10 cm. At curtained time intervals, the buried films were taken out from the soil and rinsed with water and methanol. The film samples were dried in a hot air oven at 60 °C for 24 h and weighed. The degradation of the films was monitored for up to 60 days and assessed using SEM. The percentage of weight loss was calculated by the following equation:

$$\text{Weight loss (\%)} = [(W_O\text{-}W_F)W_O] \times 100$$

where W_O and W_F were the dried weights before and after biodegradation test, respectively.

3.7 Application of the film as a freshness indicator

3.7.1 Antioxidant activity

The antioxidant activity of the fabricated films was analyzed by a 2,2-diohenyl-1-1 picrylhydrazyl (DPPH) radical scavenging assay. For the DPPH testing, 0.24 mM of DPPH was prepared by dissolving in 99.9% ethanol. The film samples (1 cm × 1cm) were immersed in 1 mL of DPPH solution and kept in the dark for 30 min at room temperature. Then, 200 µL of DPPH solution treated with each film was withdrawn and transferred into a well of 96-well plate. These solutions were measured for the absorbance at 517 nm and the DPPH solution without film sample was also measured and used as a control. The DPPH free radical scavenging capacity of film samples was presented as DPPH inhibition and calculated by the following equation (Akhila et al., 2023):

$$\text{DPPH inhibition (\%)} = \frac{A_{DPPH} - A_{extract}}{A_{DPPH}} \times 100$$

where A_{DPPH} is the absorbance of DPPH solution as a control and $A_{extract}$ is the absorbance of DPPH solution containing film.

3.7.2 Stability of the color

The color stability of the samples was investigated after keeping them at room temperature and conditions for 28 days. Their color changes were assessed using a WR-10 colorimeter (Shenzhen Wave Optoelectronics Technology) (Q. Wang et al., 2022).

3.7.3 Application for food freshness detection

The films were evaluated as an indicator for monitoring of food freshness. Fresh water shrimp was used as a fresh food sample. Each film was attached under the cover lid of a glass container containing 3 shrimps (approximate weight of 30 g) and kept at room temperature for 3 days. Color changes of the films were evaluated using a WR-10 colorimeter (Shenzhen Wave Optoelectronics Technology) and the photographs were taken (Sobhan, Muthukumarappan, & Wei, 2022).

CHAPTER 4
RESULTS AND DISCUSSION

4.1 Characterization of KC/PV films

The prepared films of κ-carrageenan and poly(vinyl alcohol) in varying blend ratios, 40KC/60PV, 50KC/50PV, and 60KC/40PV, were obtained by solution casting method. Digital images of the blend films are shown in Figure 4-1. These films were homogeneous, transparent and colorless with smooth surface, indicating compatibility between κ-carrageenan and poly(vinyl alcohol).

40KC/60PV 50KC/50PV 60KC/40PV

Figure 4-1 Digital images of the blend films.

4.1.1 ATR-FTIR of KC/PV films

The characteristic functional groups of the homopolymers and blend films were analyzed by ATR-FTIR spectroscopy and shown in Figure 4-2. The FTIR spectrum of κ-carrageenan and poly(vinyl alcohol) exhibited both common and specific absorption peaks around 3330 cm^{-1} and 2900 cm^{-1}, which were assigned to the vibrational stretching of hydroxyl groups and the stretching frequency of C-H bonding (Figure 4-2a). The κ-carrageenan film showed characteristic bands at 1225, 1120, 927 and 842 cm^{-1} which could be assigned to the ester sulfate asymmetric stretching, C-O stretching, 3, 6-anhydrogalactose and D-galactose-4-sulfate stretching, respectively (Lapwanit, Sooksimuang, & Trakulsujaritchok, 2018; Sukhlaaied & Riyajan, 2013). In FTIR spectra of poly(vinyl alcohol), the bands at 1720, 1450, 1320 and 1018 cm^{-1}were due to the C=O stretching of non-hydrolyzed vinyl acetate groups, C-H bending, O-H bending and C-O stretching, respectively

(Pipattanawarothai & Trakulsujaritchok, 2020; Sukhlaaied & Riyajan, 2013). For the KC/PV blend films (Figure 4-2b), the spectra showed absorption bands inherited from their homopolymers with small shifting on the intensities due to the interactions between both polymers.

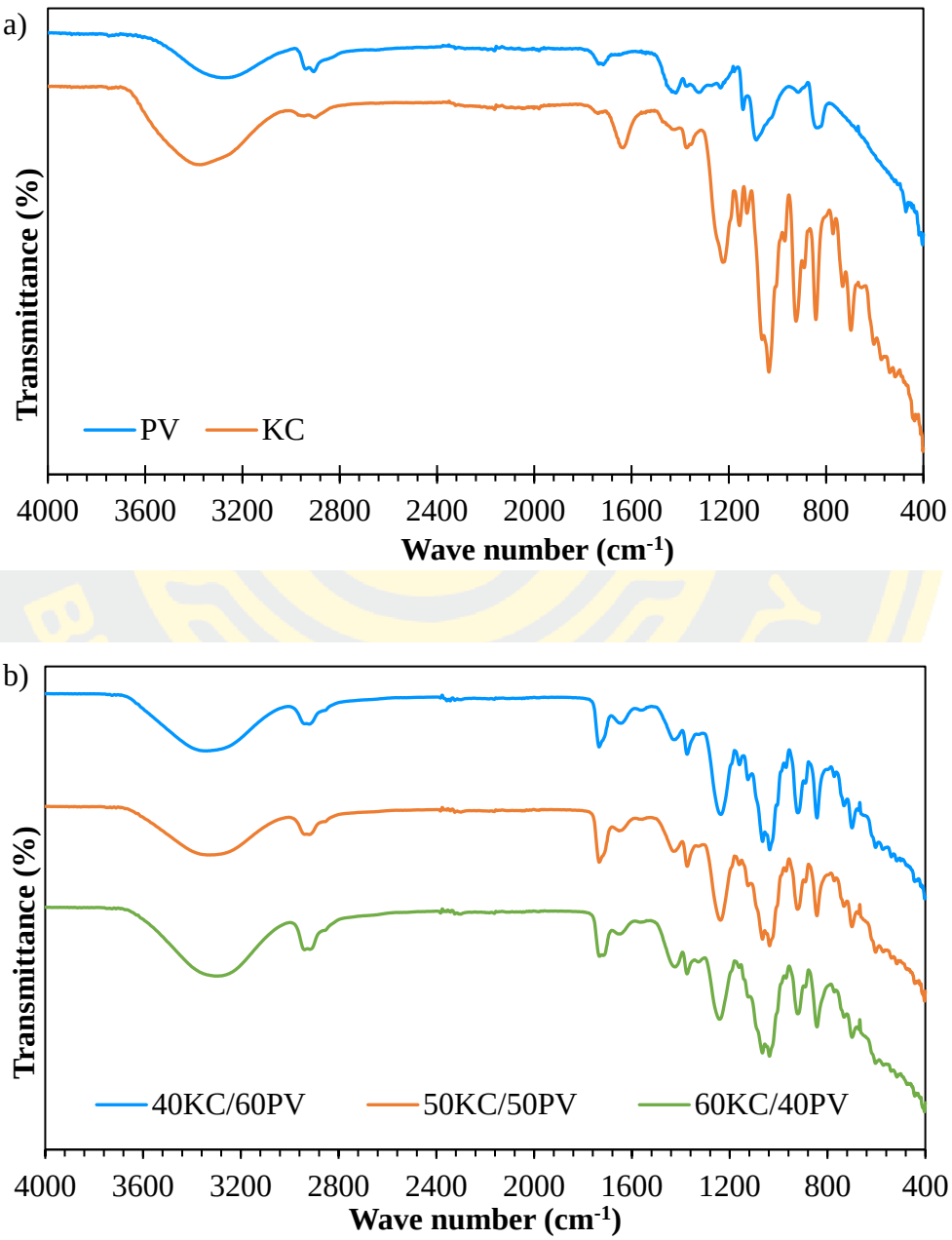

Figure 4-2 FTIR spectra of films a) homopolymers and b) the blends containing different homopolymer ratios.

4.1.2 Effect of compositions on properties of the KC/PV films

4.1.2.1 Solubility and swelling of the KC/PV films.

The swelling ratio and solubility of the KC/PV films were determined in an aqueous medium and the results are shown in Figure 4-3. Both swelling ratio and %solubility increased with increasing the κ-carrageenan component. The swelling ratios obtained from 40KC/60PV, 50KC/50PV and 60KC/40PV films at 30 min of the test were 8.6, 12.0 and 14.6 g/g, respectively. %Solubility of the films after 360 min immersion in distilled water were 54.0, 60.2, and 69.1% for the 40KC/60PV, 50KC/50PV and 60KC/40PV, respectively. Comparing with their homopolymers which were completely dissolved after the tests, it was observed that the blends showed more water resistance due to the macromolecular interactions between their polymeric constituents such as hydrogen bonding and chain entanglement. The results correspond with those of moisture content in which the hydrophilicity of κ-carrageenan had strong influence on the blend and governed their water resistance. As a matter of fact, comparing between the two homopolymers, κ-carrageenan was easier to dissolve in water (S. Wang, Ren, Li, Sun, & Liu, 2014).

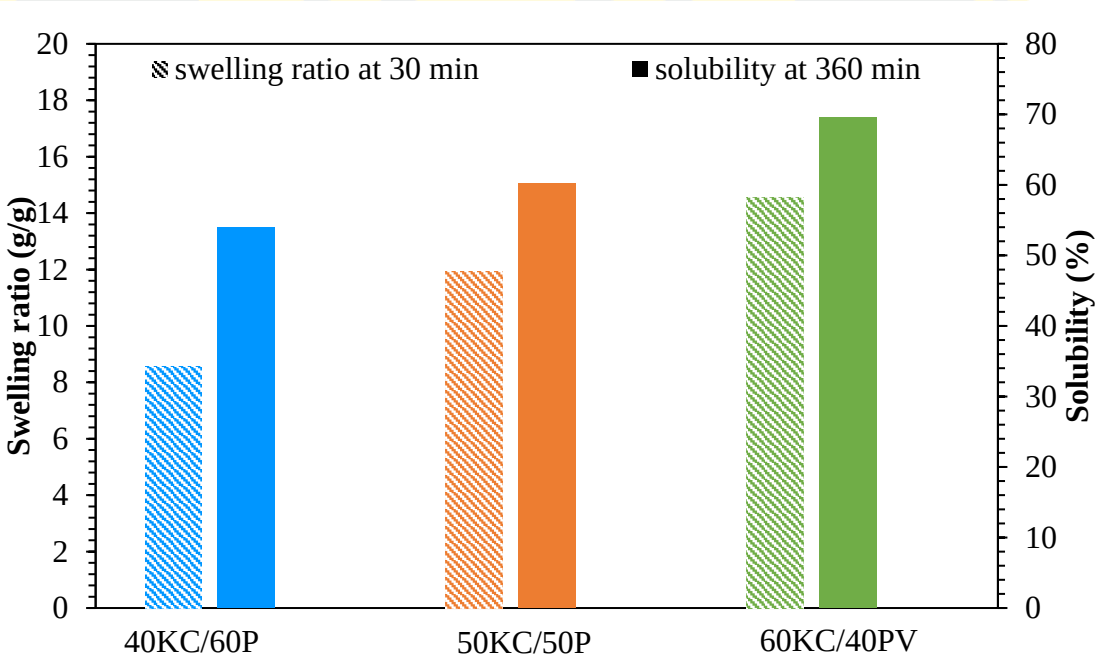

Figure 4-3 Swelling ratio and %solubility of the blends containing different homopolymer ratios.

4.1.2.2 Moisture content of the KC/PV films

The moisture contents of KC/PV films are presented in Figure 4-4. Among the three blend films, the 60KC/40PV showed the highest moisture content (11.31 and 15.52% at 3 and 24 h, respectively) as compared to the lowest values obtained from the 40KC/60PV (2.16 and 7.14 % at 3 and 24 h, respectively). Increasing the content of κ-carrageenan led to an increase in %moisture adsorbed into the samples which could be explained by hydrophilicity of κ-carrageenan that facilitated the intermolecular interactions between water molecules and the polymeric film (Qin, Liu, Zhang, & Liu, 2020).

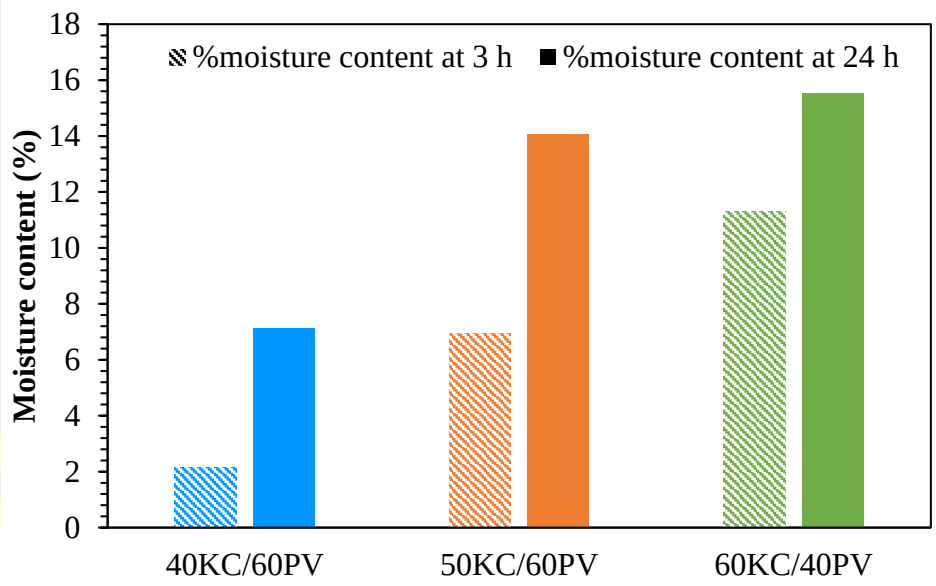

Figure 4-4 Moisture content of the blends containing different homopolymer ratios.

4.1.2.3 Mechanical properties of the KC/PV films

The mechanical properties of the KC/PV films with various homopolymer ratios are represented in Table 4-1. Incorporation of poly(vinyl alcohol) into the κ-carrageenan matrix resulted in an increase in tensile properties. Similar results have been reported in the literature (Y. Liu et al., 2019). Among the three compositions, the 40KC/60PV exhibited ultimate values of mechanical strength with tensile strength of 24.68 MPa, elongation at break of 3.55% and Young's modulus of 8.67 MPa. Improvement in mechanical properties of the films was achieved by blending κ-carrageenan with poly(vinyl alcohol). Considering the mechanical strength and water

resistance character of the samples, the 40KC/60PV blend was chosen for further investigation on the effects of hybrid organic-inorganic crosslinking on the physicochemical properties in next section.

Table 4-1 Mechanical properties of the KC/PV films

Samples	Tensile strength (MPa)	Elongation at break (%)	Young's Modulus[a] (MPa)
40KC/60PV	24.68	3.55	8.67
50KC/50PV	11.61	2.97	3.48
60KC/40PV	6.20	1.27	2.91

[a] Young's Modulus at 1% elongation

4.2 Characterization of sol-gel crosslinked KC/PV-T films

In this study, the 40KC/60PV blend film was chosen for the investigation on enhancement of its properties through the sol-gel process. The sol-gel process was employed to prepare hybrid organic-inorganic crosslinked films and improved their physicochemical properties. The chemical reactions of the sol-gel process consisting of hydrolysis and condensation are shown in Figure 4-5.

Hydrolysis: $Si\text{-}(OR)_4 + H_2O \rightarrow HO\text{-}Si\text{-}(OR)_3 + ROH$

Polycondensation: $(RO)_3\text{-}Si\text{-}OH + HO\text{-}Si\text{-}(OR)_3 \rightarrow (RO)_3\text{-}Si\text{-}O\text{-}Si\text{-}(OR)_3 + H_2O$

$(RO)_3\text{-}Si\text{-}OH + RO\text{-}Si\text{-}(OR)_3 \rightarrow (RO)_3\text{-}Si\text{-}O\text{-}Si\text{-}(OR)_3 + ROH$

and/or $(RO)_3\text{-}Si\text{-}OH + HO\text{-}[polymer] \rightarrow (RO)_3\text{-}Si\text{-}O\text{-}[polymer] + H_2O$

R : alkyl group

The sol-gel process could be described as two steps. The first step involved the hydrolysis of the ethoxysilane groups in tetraethyl orthosilicate (TEOS), an inorganic precursor, which were hydrolyzed and the Si-OH pendants were formed. Then, the polycondensation proceeded resulting in formation of -Si-O-Si- covalent crosslinking of the organic-inorganic hybridized networks polymer chains (Pipattanawarothai &

Trakulsujaritchok, 2020). These processes played an important role in fabricating crosslinked films via hydrolysis and polycondensation. The changes in the physicochemical properties of the hybrid films were reported in the next section.

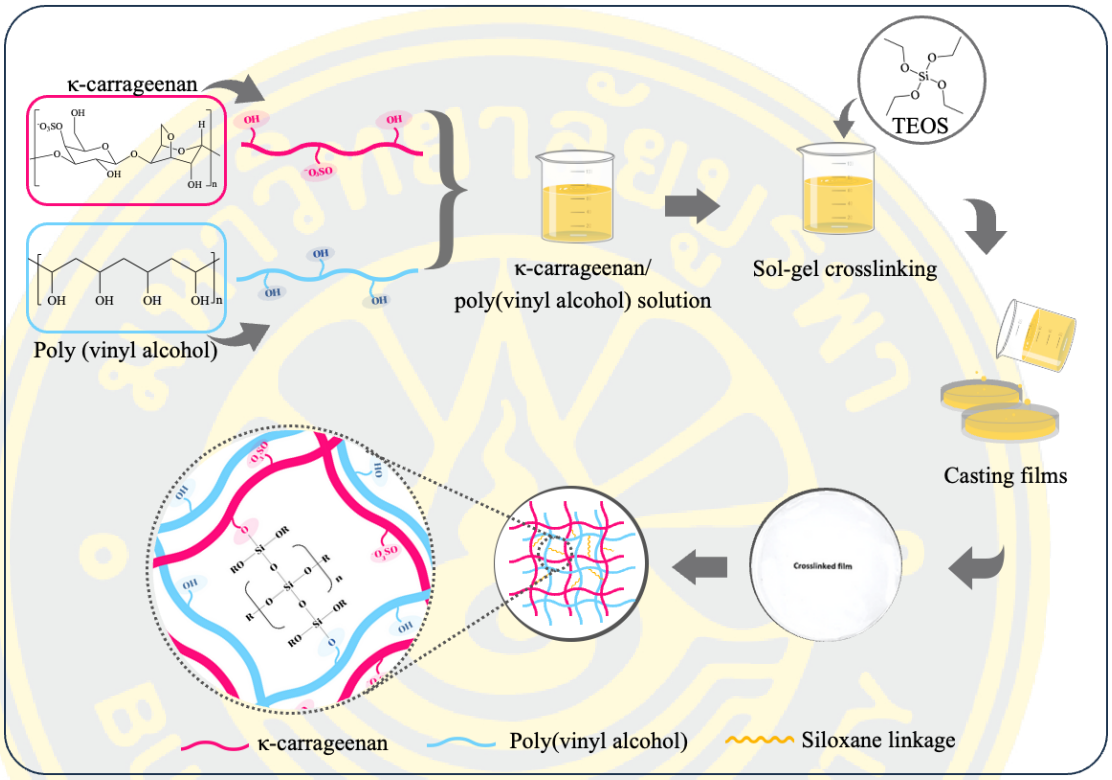

Figure 4-5 Preparation scheme for sol-gel crosslinking of the hybrid KC/PV-T films.

4.2.1 ATR-FTIR of the crosslinked 40KC/60PV-T films

The success of sol-gel synthesis and the occurrence of organic-inorganic crosslinking in the hybrid KC/PV-T films through the Si-O-Si linkage could be confirmed by FTIR spectroscopy. The ATR-FTIR spectra ranging from 1600 to 400 cm^{-1} of the sol-gel crosslinked film, 40KC/60PV-T45, comparing with its linear blend, 40KC/60PV, are shown in Figure 4-6. The new bands of C-H bending (TEOS ethoxy groups) at 1330 cm^{-1} and those of the siloxane linkage formation in the 40KC/60PV-T45 were observed at 1140 and 820 cm^{-1} corresponding to the asymmetric stretching bands and symmetric stretching band of Si-O-Si, respectively (Korbag & Mohamed Saleh, 2016; Pipattanawarothai & Trakulsujaritchok, 2020)

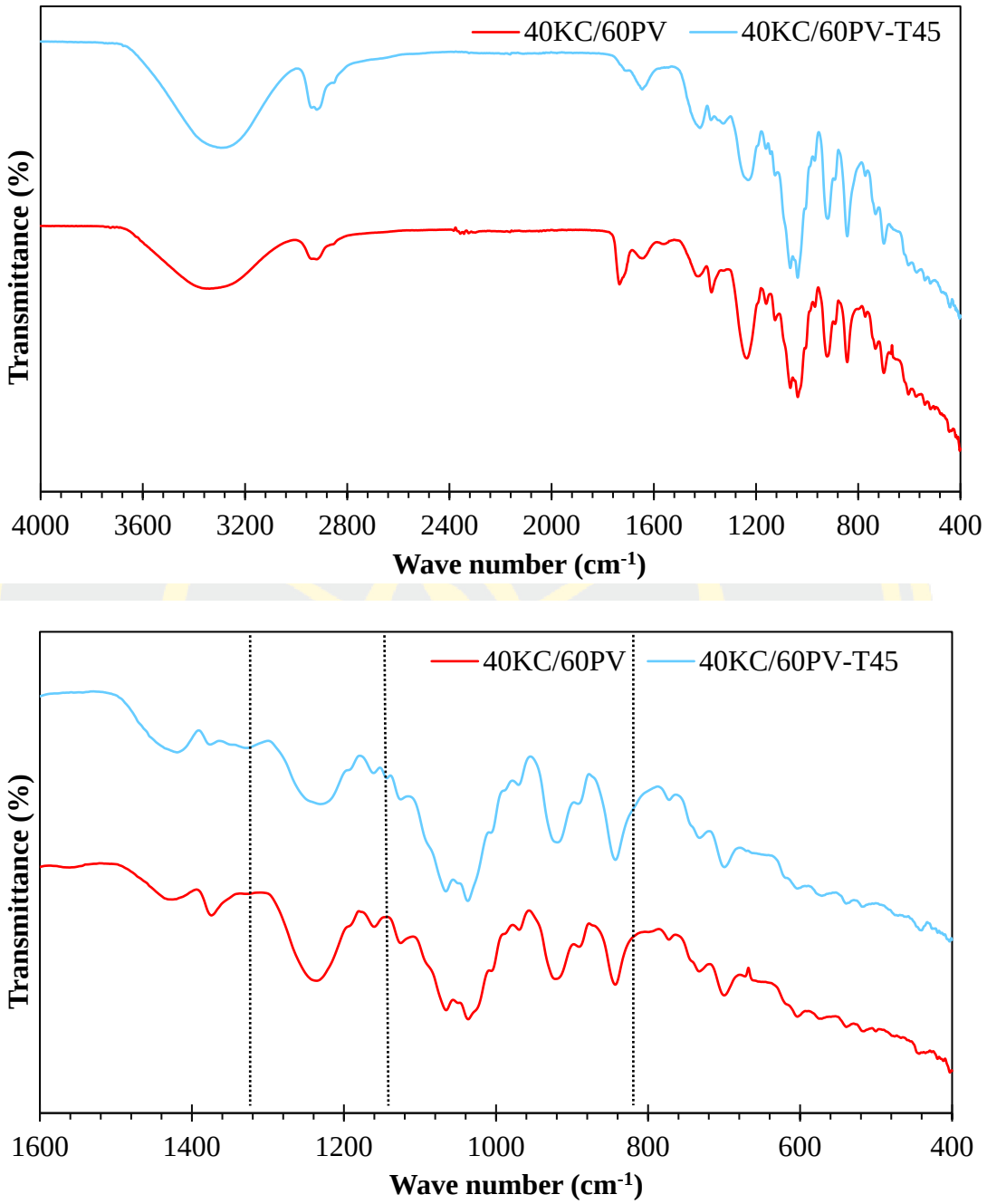

Figure 4-6 ATR-FTIR spectra of the linear blend (40KC/60PV) and the crosslinked hybrid films (40KC/60PV-T45).

4.2.2 Properties of the crosslinked 40KC/60PV-T films

To study the effects of the sol-gel crosslinking on the mechanical properties of the film. Tensile properties of the 40KC/60PV-T45 were tested and the results are presented in Table 4-2. The 40KC/60PV-T45 film had tensile strength of 43.20 MPa,

elongation at break of 7.47 % and Young's modulus of 11.94 MPa, which were higher than those of the film without the addition of the sol-gel precursor. The strength and flexibility of the hybrid 40KC/60PV-T45 films were improved through organic-inorganic crosslinking.

The swelling test of the 40KC/60PV and the 40KC/60PV-T45 films was performed in an aqueous medium and the swelling ratios are displayed in Table 4-2. Swelling ratio at 30 min decreased with the incorporation of crosslinking agent in polymer blend. Swelling ratio of the crosslinked sample was 6.07 g/g as compared the value of 8.55 g/g obtained from the 40KC/60PV blend. The 40KC/60PV-T45 showed 43.85% weight remaining after 300 min swelling test in water which was higher than the value measured from the 40KC/60PV. These results confirmed that the polymeric blend was successfully crosslinked with TEOS through the sol-gel approach.

Table 4-2 Properties of the linear blend and the crosslinked film.

Samples	Tensile strength (MPa)	Elongation at break (%)	Young's modulus[a] (MPa)	Swelling ratio[b] (g/g)	Weight remaining[c] (%)
40KC/60PV	24.68	3.55	8.67	8.55	34.72
40KC/60PV-T45	43.20	7.47	11.94	6.07	43.85

[a] Young's Modulus at 1% elongation

[b] Swelling ratio at 30 min

[c] Weight remaining at 300 min

4.2.3. SEM-EDX of the crosslinked 40KC/60PV-T films

Scanning electron microscopy was used to examine the microstructure of the blend and crosslinked films. The SEM micrographs of the surfaces and the EDX analysis of both films are shown in Figure 4-7. The 40KC/60PV film before sol-gel synthesis showed a smooth surface, indicating all components were homogeneous. The slightly coarse morphology on the surface of 40KC/60PV-T45 film could be due to the associated formation of hybrid organic-inorganic network, which was confirmed by their EDX elemental compositions. EDX analysis of 40KC/60PV-T45 showed Si-elemental content of the crosslinking agent added into the reaction.

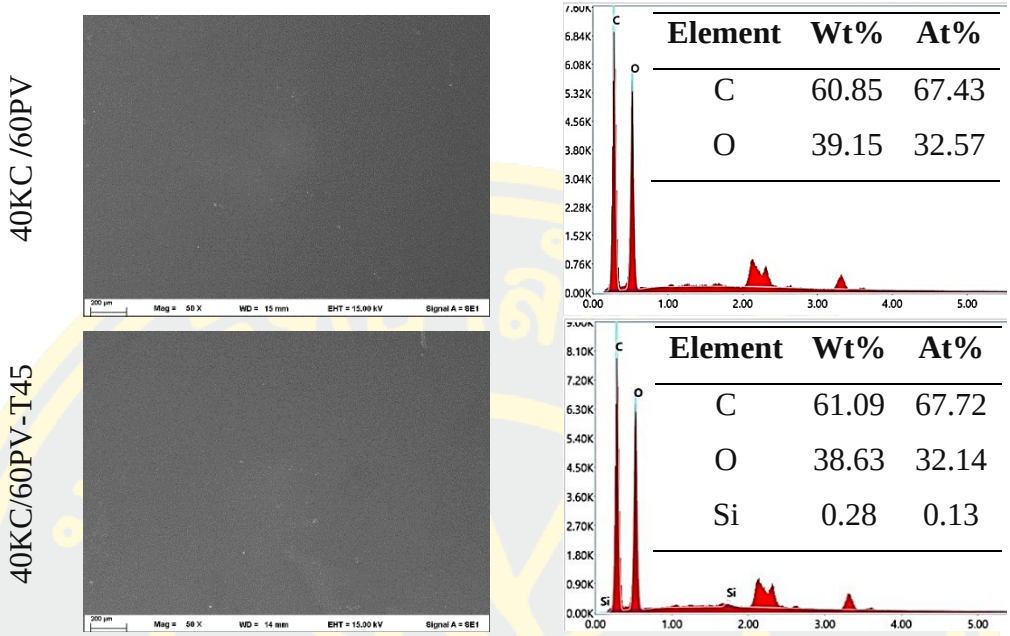

Figure 4-7 SEM-EDX analysis of the linear blend and the crosslinked films.

4.3 Characterization of the crude extract

4.3.1 pH-responsive character

The natural extract obtained from *Ruellia squarrosa* (Fenzi) Cufod. or mexican petunia flowers possessed a distinct pH-responsive character. The color changes of the crude extract in different pH solutions are displayed in Figure 4-8. The crude extract showed varied in color from pink to light pink under acidic conditions and greenish to yellowish-brown under alkaline conditions. The changes in color were caused by anthocyanin compounds that exhibited varied structural transformations as pH condition was changed. Anthocyanins in acidic condition were in the forms of flavylium cations. At pH 1, the flavylium cations (intense pink color) were predominant. At pH 2-6, the concentration of cation forms was lessened, as a result, the faded in pink was observed. At pH values between 7 and 8, anthocyanins were in the predominant forms of quinoidal blue and the solution color was green with a tinge of blue. When the pH was increased to the values between 9-10, anthocyanins were the mixture forms of two species, the anhydro base and chalcone. At pH values higher than 11, the compound in the form of chalcone was dominant in which the color was obviously seen as yellow (Supalert, 2021). The pH influences upon chemical forms of

anthocyanin were investigated and reported by Castaneda-Ovando and co-workers as shown in Figure 4.9 (Castañeda-Ovando, Pacheco-Hernández, Páez-Hernández, Rodríguez, & Galán-Vidal, 2009).

The pH-responsiveness of the crude extract under variations in pH solutions from 1 to 12 was further monitored by UV–visible spectroscopy and the results are shown in Figure 4-10. The UV-Vis spectra of the crude extract showed the maximum absorption peak shifting from around 533 nm (under acidic conditions) to 615 nm (under alkaline conditions) and the solution exhibited a color change from pink to green and yellow. These results were corresponded with those reported by (Forghani et al., 2022; Q. Wang et al., 2022).

Figure 4-8 Color variations of the crude extract under different pH solutions (pH 1 to 12).

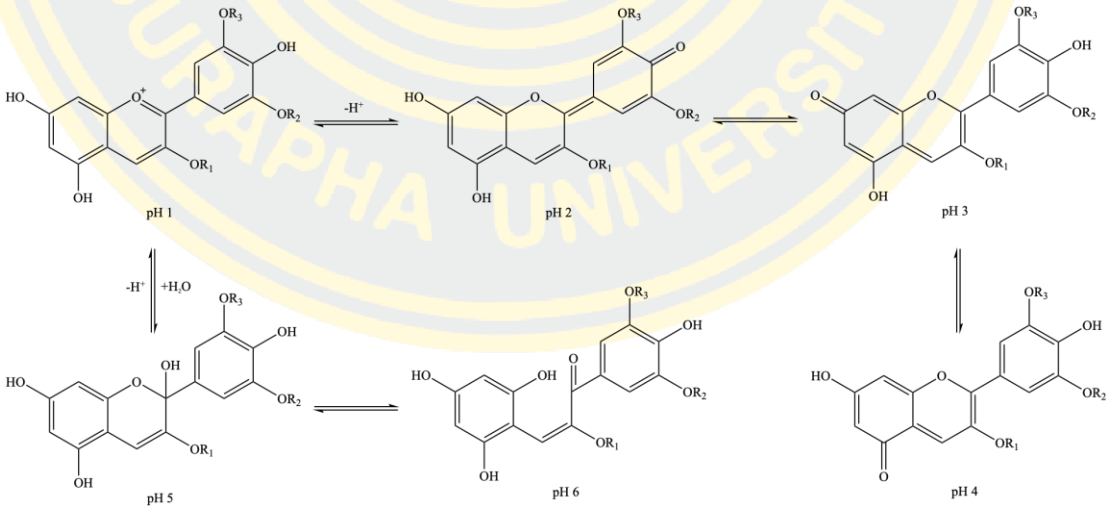

Figure 4-9 Anthocyanin chemical forms depending on environmental pH.

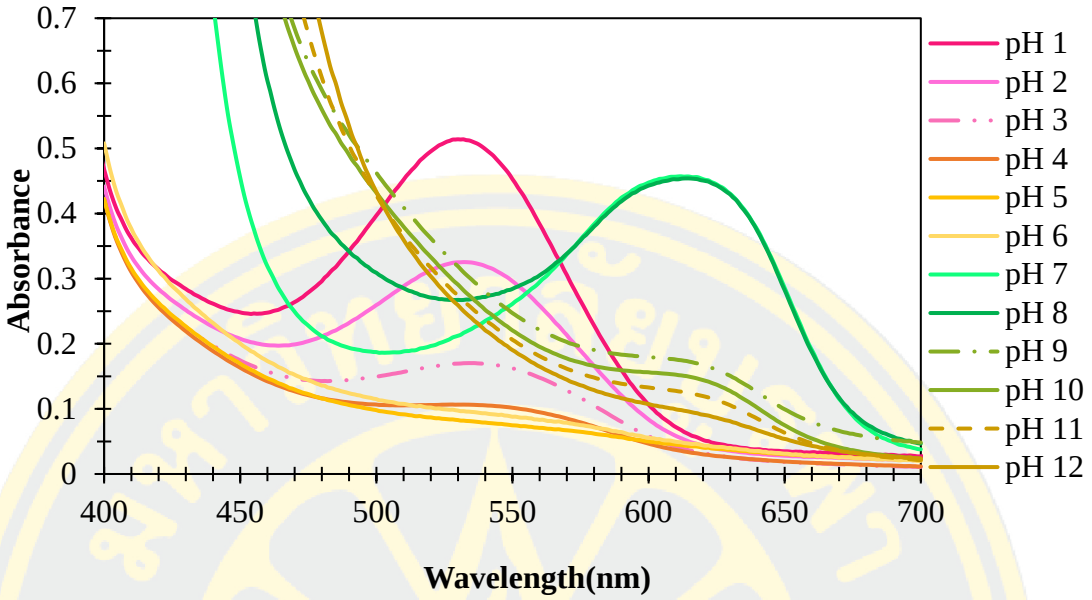

Figure 4-10 UV-visible absorption spectrum of the crude extract under different pH solutions.

4.3.2 Evaluation of antioxidant activity and total phenolic content

Phytochemical studies on the crude extract exhibited the presence of various bioactive compounds, as shown in Table 4-3. The total phenolic, total *ortho*-hydroxyphenolic and total anthocyanin contents of the crude extract were analyzed using the Folin-Ciocalteu, ferric chloride ($FeCl_3$) and pH-differential methods, respectively. The values of 167.44 ± 4.85 mg GAE/g extract, 24.17±1.53 mg GAE/g extract and 52.77 ± 3.53 mg CGE/100 g of DW were found for total phenolic, total *ortho*-hydroxyphenolic and total anthocyanin contents, respectively, which were approximately close to the results obtained from other researchers (Freyre, 2015; Sianturi, Trisnawati, Koketsu, & Suryanti, 2023).

Additionally, the antioxidant activity of the crude extract of mexican petunia flowers was determined by the DPPH assay and percentage of inhibition are presented in Table 4-4. It was revealed that %DPPH inhibition or scavenging activity of the extract increased with its concentrations. The highest antioxidant activity was observed at 1.25 mg/ml concentration. The above results suggested that the crude extract of mexican petunia flowers contained both phenolic and anthocyanin compounds, which contributed to the antioxidant activity. Therefore, the crude extract

could be utilized for the development of active packaging films possessing the functions of antioxidant activity and real-time monitoring of food freshness.

Table 4-3 Bioactive compounds estimation of the crude extract.

Bioactive compounds	
Yield (%) of crude extract	13.03 ± 1.57
TPC (mg GAE/g extract)	167.44 ± 4.85
TOHPC (mg GAE/g extract)	24.17 ± 1.53
TAC (mg CGE/100 g DW)	52.77 ± 3.53

Table 4-4 Antioxidant activity of the crude extract at different concentrations.

Concentrations (mg/mL)	DPPH inhibition (%)
1.25	91.17±0.10
0.63	90.62±0.75
0.31	83.31±3.19
0.16	46.88±3.63

4.4 Characterization of the pH sensitive films

4.4.1 Appearance of the pH sensitive films

From the optimization of homopolymer ratio and the investigation of sol-gel crosslink on properties of the films, it was revealed that the 40KC/60PV-T45 demonstrated outstanding characters. This film was chosen for further development by incorporation of crude extract comprising anthocyanins obtained from mexican petunia flowers to fabricate pH sensitive films. The digital images of the films with and without crude extracts are shown in Figure 4-11. The pH sensitive films with varied crude extract content, 40KC/60PV-T45-5R, 40KC/60PV-T45-10R, 40KC/60PV-T45-20R, and 40KC/60PV-T45-30R, were yellowish to brownish in color. The coloration of the indicator films depends on the concentration of crude extracts in the polymeric film.

a) b) c) d) e)

Figure 4-11 Digital images of the film with and without crude extract a) 40KC/60PV-T45-0R, b) 40KC/60PV-T45-5R, c) 40KC/60PV-T45-10R, d) 40KC/60PV-T45-20R and e) 40KC/60PV-T45-30R.

4.4.2 ATR-FTIR of the pH sensitive films

The ATR-FTIR spectroscopy was employed to characterize the functional groups and intermolecular interactions of the films. The FTIR spectra of the crude extract containing anthocyanins (Figure 4-12), the films with and without crude extract are shown in Figure 4-13. The pH sensitive films and crude extract showed characteristic peaks of the hydroxyl stretching vibrations around 3200-3400 cm^{-1} and the C-H stretching around 2900 cm^{-1}. In the spectrum of crude extract (Figure 4-13a), the bands at 1738, 1605, 1445 and 1050 cm^{-1} could be corresponding to the stretching vibration of C=O, stretching vibration of aromatic ring C=C, stretching vibration of C-C bonding and deformation of aromatic ring C-H bonding, respectively (Forghani et al., 2022; Y. Liu et al., 2020). FTIR spectra of the films incorporated with crude extract (Figure 4-13b) showed a new shoulder around 1606 cm^{-1} which was the main characteristic of the extract. Compared with the 40KC/60PV-T45-0R, the peak at 1640 cm^{-1} assigned to polymer bound water of carrageenan gradually became broader and shifted to lower wavenumbers with increasing the crude extract content. These results were ascribed to the interaction between polymeric matrix and crude extract through hydrogen bonds (Chen et al., 2023).

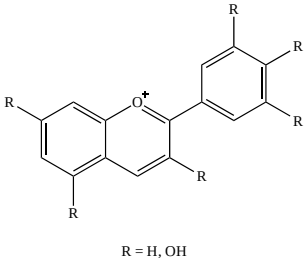

Figure 4-12 General structure of anthocyanin.

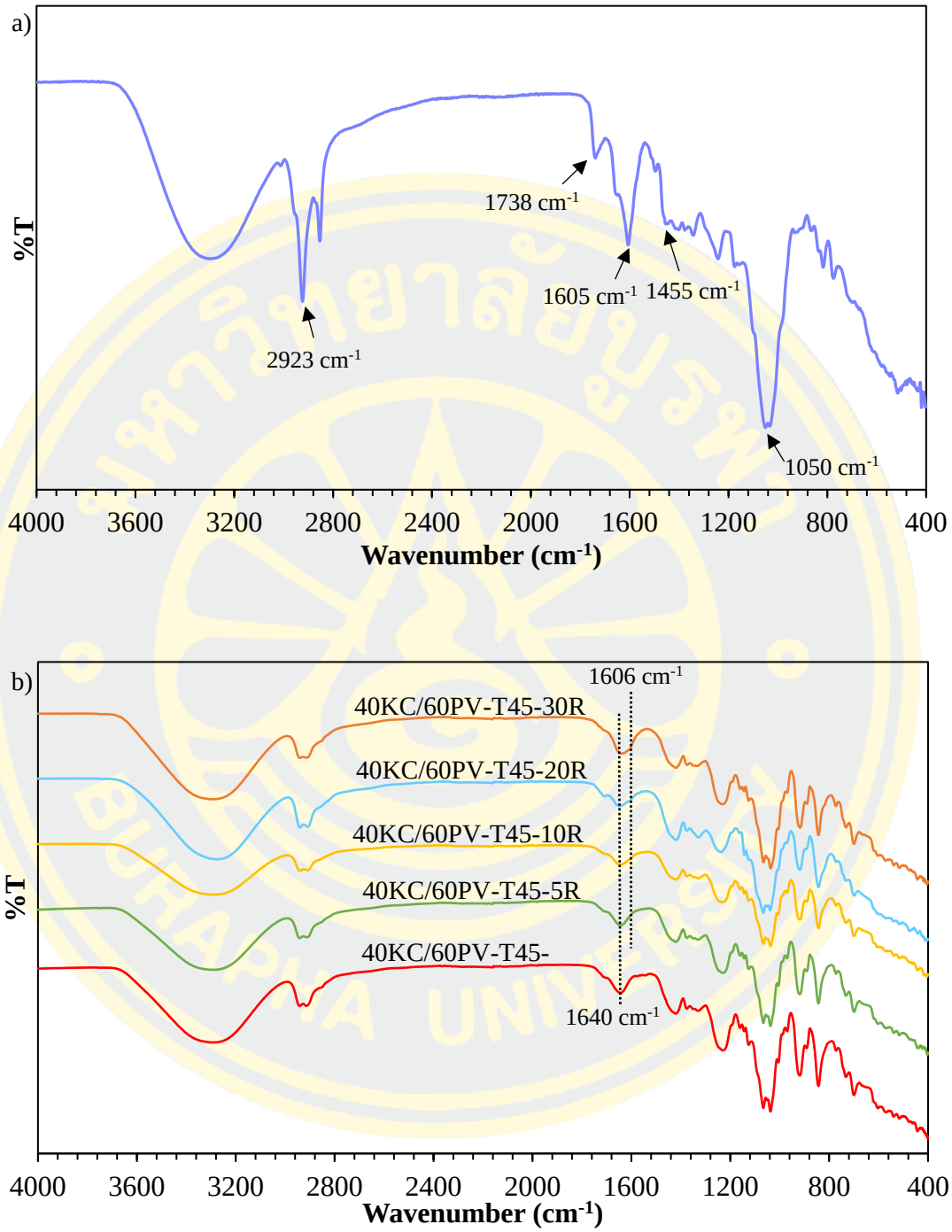

Figure 4-13 FTIR spectra of a) the crude extract and b) films with and without crude extract.

4.4.3 Morphology of the pH sensitive films

Scanning electron microscope (SEM) was used to investigate surface morphology of the fabricated films and the micrographs are presented in Figure 4-14. From the analysis at high magnification, the film without crude extract (40KC/60PV-T45-0R) displayed smooth surface morphology. The films loaded with crude extract showed rougher surface without phase separation, indicating the compatibility between the crude extract and the polymeric blend.

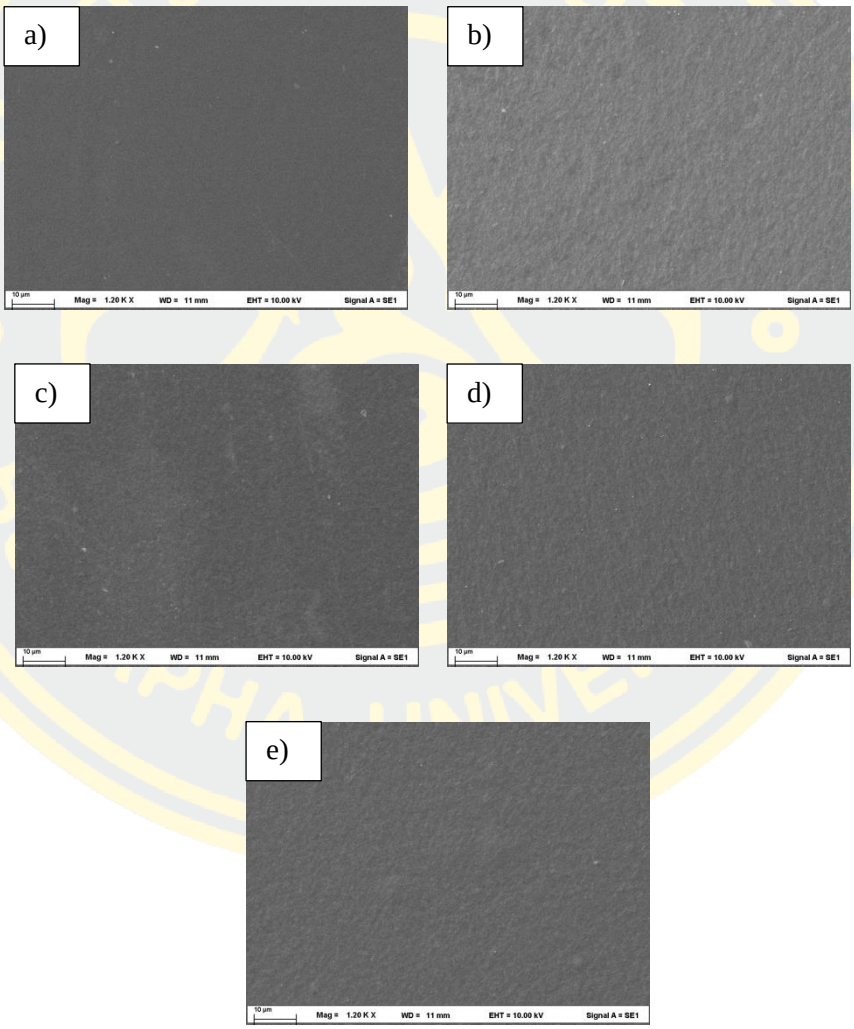

Figure 4-14 SEM micrographs of the films with and without crude extract. (a) 40KC/60PV-T45-0R, b) 40KC/60PV-T45-5R, c) 40KC/60PV-T45-10R, d) 40KC/60PV-T45-20R and e) 40KC/60PV-T45-30R)

4.4.4 Mechanical properties of the pH sensitive films

The mechanical properties of films with and without the crude extract are presented in Table 4-5. The values of tensile strength, elongation at break and Young's Modulus of the 40KC/60PV-T45-0R were 71.18 ± 0.67 MPa, 8.17±0.97 % and 17.03 ± 0.33 MPa, respectively. Addition of the crude extract into the 40KC/60PV-T45-R film resulted in a decrease in tensile strength and Young's Modulus. On the other hand, the values of elongation at break were enhanced as the concentration of crude extract was increased. The crude extract affected mechanical properties of the films similar to that of a plasticizer. The decrease in tensile strength could cause by anthocyanins that interrupted of inter and intramolecular interactions between polymer molecules. Similar behaviors were reported in the literature (Forghani et al., 2022). Figure 4-15 shows the 40KC/60PV-T45-5R films that were easily bent, folded, twisted and stretched confirming the flexibility of the fabricated film.

Table 4-5 Mechanical properties of the films with and without the crude extract.

Samples	Tensile strength at break (MPa)	Elongation at break (%)	Young's Modulus[a] (MPa)
40KC/60PV-T45-0R	71.18±0.67	8.17±0.97	17.03±0.33
40KC/60PV-T45-5R	62.45±6.32	11.71±0.28	13.52±0.86
40KC/60PV-T45-10R	59.97±2.66	12.71±0.50	12.78±0.38
40KC/60PV-T45-20R	49.39±3.10	12.44±2.17	10.12±0.23
40KC/60PV-T45-30R	46.00±1.38	14.75±2.46	8.86±1.20

[a] Young's Modulus at 2.5% elongation

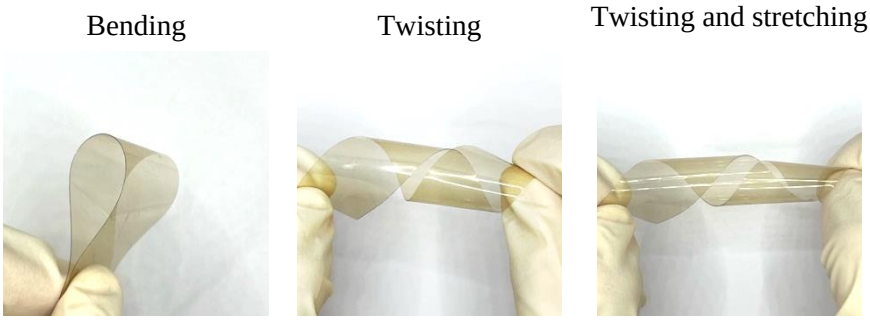

Figure 4-15 Digital photographs of the 40KC/60PV-T45-5R film under deformation forces.

4.4.5 Swelling of the pH sensitive films

The swelling ratios of films loaded with different rations of crude extract were examined in an aqueous medium and the results are shown in Figure 4-16. Incorporation of the extract into the polymer matrix resulted in a decrease in the swelling ratio. The 40KC/60PV-T45-30R composing the highest amount of crude extract presented the lowest swelling ratio. The decrease in swelling may be attributed to the occurrence of hydrogen bonding between the hydroxyl groups of crude extract and the polymer chains. Similar result was observed in the literature (Singh et al., 2021).

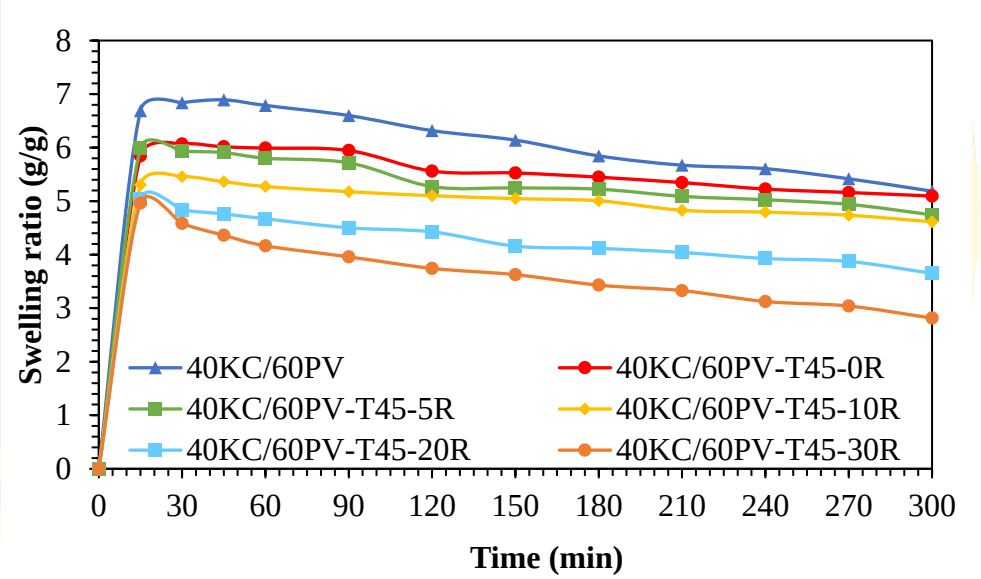

Figure 4-16 The swelling ratios of the films with and without the crude extract.

4.4.6 Water vapor transmission rate of the pH sensitive films

Water vapor transmission rate (WVTR) of the prepared films was determined and the results are shown in Table 4-6. The 40KC/60PV-T45-0R film had a WVTR value of 5.47 ± 0.91 g/m^2·h. The films loaded with crude extract showed decreasing of WVTR values with increasing content of the crude extract. For the 40KC/60PV-T45-5R, the value significantly decreased to 4.28 ± 0.31 g/m^2·h. The reduction in WVTR values of the indicator films could be attributed to the intermolecular interaction between polymeric chains and anthocyanin component, resulting in a compact matrix with lower amount of free hydroxyl groups available for interaction with water vapor.

These results demonstrated that the films containing the crude extract exhibited an enhanced barrier property. A decrease in WVTR values was previously reported for the *Jacaranda cuspidifolia* extract loaded chitosan/poly(vinyl alcohol) composite films (Amaregouda et al., 2022) and that of the *Ipomoea coccinea* extract filled poly(vinyl alcohol)/guar gum films (Akhila et al., 2023).

Table 4-6 Water vapor transmission rate of the films with and without the crude extract.

Samples	WVTR ($g/m^2 \cdot h$)
40KC/60PV-T45-0R	5.47±0.91
40KC/60PV-T45-5R	4.28±0.31
40KC/60PV-T45-10R	3.89±0.36
40KC/60PV-T45-20R	3.97±0.70
40KC/60PV-T45-30R	3.98±0.59

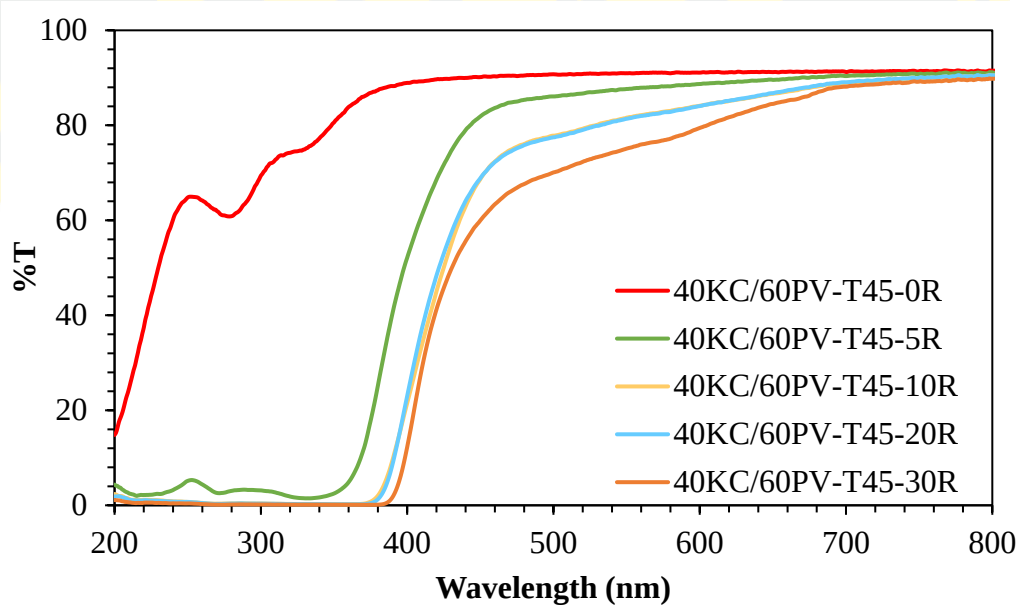

Figure 4-17 UV-Vis transmittance of the films with and without the crude extract.

4.4.7 UV-blocking of the pH sensitive films

The UV light blocking performance of films is a preferred characteristic in food packaging materials due to UV light can lead to oxidation and degradation of

packaged foods. The UV barrier property of the prepared films was analyzed using UV-Vis spectroscopy and the transmittance spectra in the range of 200-800 nm are presented in Figure 4-17. The 40KC/60PV-T45-0R film without the crude extract showed poor UV blocking performance while those incorporated with the crude extract exhibited significantly improved light barrier. Adding the crude extract into the polymer matrix effectively blocked the UV light in the range of 200-390 nm. The 40KC/60PV-T45-30R completely blocked the UV from 200 to 390 nm with 0% transmittance and obviously reduced the percentage of transmittance in the range of 390-700 nm. Similar findings were found by other researchers who worked with κ-carrageenan matrix films containing pomegranate peel extract (Y. Liu et al., 2020; Q. Wang et al., 2022).

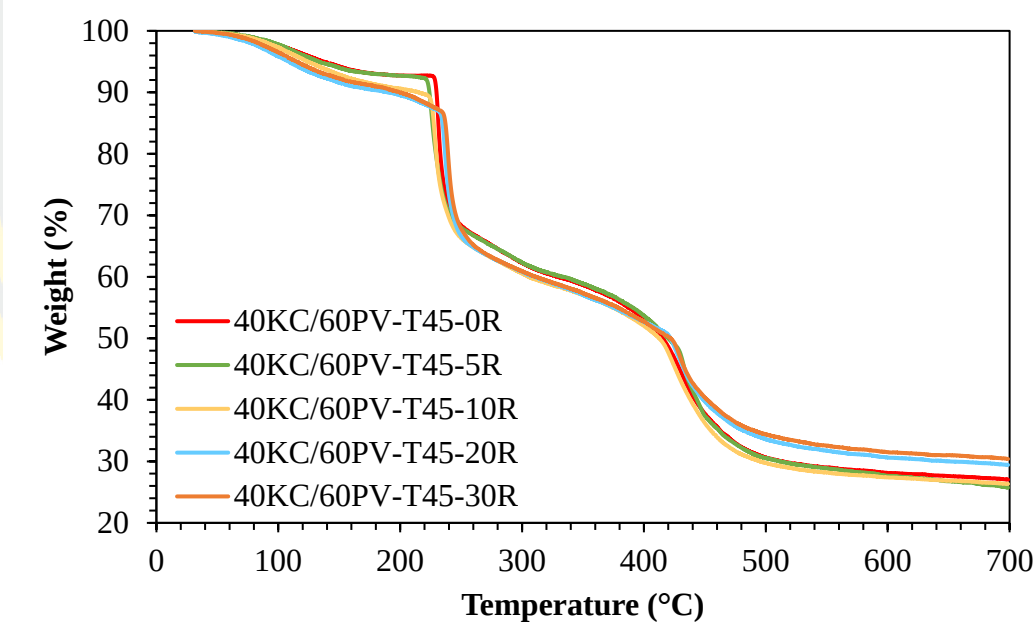

Figure 4-18 Thermal stability of the film with and without the crude extract.

4.4.8 Thermal property of the pH sensitive films

Thermal property of fabricated films was investigated by thermalgravimetric analysis and the thermograms are presented in Figure 4-18. All films exhibited three steps of weight loss through their thermal degradation. The first stage of minor weight loss observed at a temperature range below 160°C was attributed to evaporation of moisture and elimination of small molecules. The following stage in the range of 160

to 260 °C could be due to the breakdown of polymeric side chain and the major final step (260-500 °C) could cause by backbone chain scission and decomposition of linkage polymeric networks [Sabbagh et al, 2023; Forghani et al, 2022; de Jesus et al, 2023]. An increase in weight remaining over the temperature range with a high amount of residue at 700°C were observed in the thermograms of 40KC/60PV-T45-20R and 40KC/60PV-T45-30R. These results indicated the effect of anthocyanins on enhancing thermal stability of the film (Amaregouda et al., 2022).

4.4.9 Biodegradation of the pH sensitive films

The biodegradability of the films, 40KC/60PV, 40KC/60PV-T45-0R, and 40KC/60PV-T45-30R, was investigated. These films were buried in soil for 60 days and their weight loss after degradation was monitored. SEM micrographs of the samples after degradation are shown in Figure 4-19. At high magnification, all films before degradation showed slightly coarse surface morphology. After 10 days of soil burial, the degradation started resulting in irregularity and roughness of the surfaces. After 60 days, significant changes of the surface morphology as result of biodegradation were obviously observed. Rough surfaces with deep pores were caused by bioactivity of microorganisms that deteriorated the films while buried in soil. (Roy, Saha, Kitano, & Saha, 2012; Zhao et al., 2022). In addition, weight loss of the films was measured after biodegradation and results are shown in Figure 4.20. After 10 days, the percentages of weight loss obtained from 40KC/60PV, 40KC/60PV-T45-0R and 40KC/60PV-T45-30R were 9.87, 11.23 and 30.26%, respectively. After 60 days of soil burial, %weight loss values increased to 42.18, 39.41 and 64.12% for the 40KC/60PV, 40KC/60PV-T45-0R, and 40KC/60PV-T45-30R, respectively. Therefore, the fabricated films demonstrated progress in biodegradation with time, confirming that they can be considered as an environmentally friendly material.

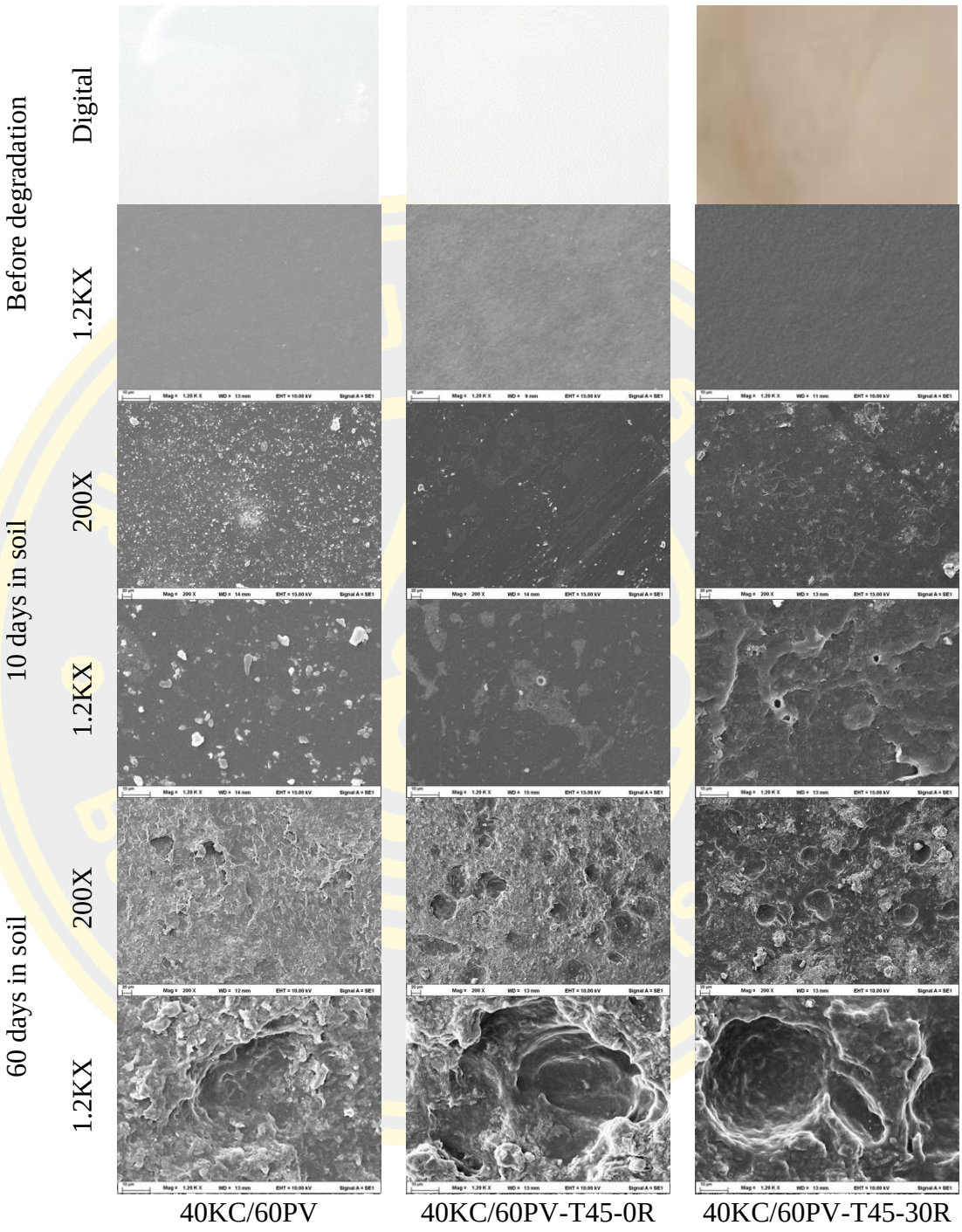

Figure 4-19 The digital photographs and SEM micrographs of the films before and after degradation.

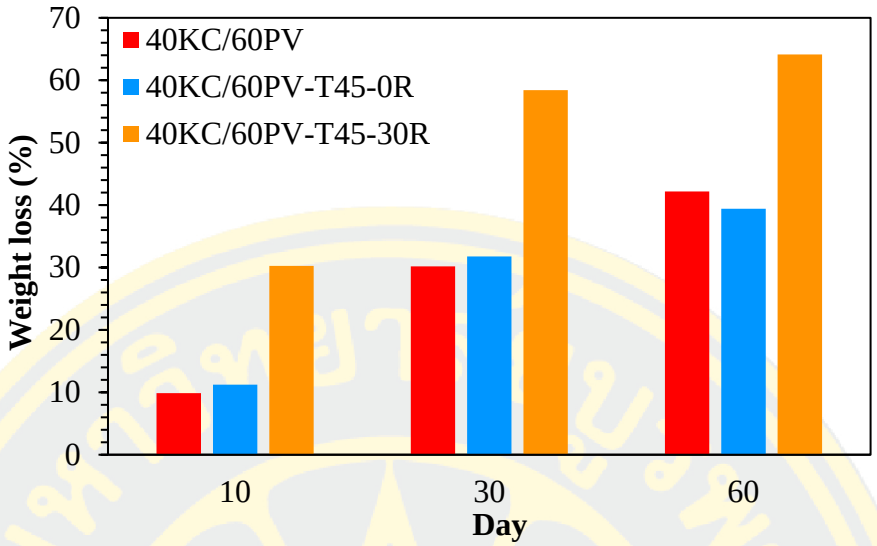

Figure 4-20 Weight loss of the films after soil degradation for 60 days.

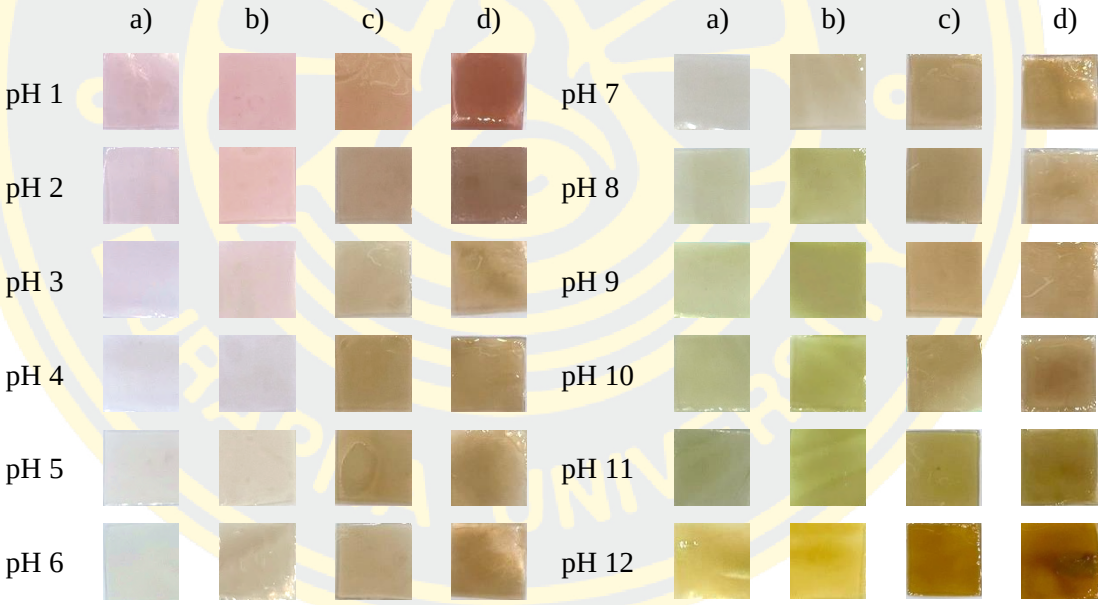

Figure 4-21 The digital photographs of pH-sensitive films after immersion in different pH solutions (pH 1-12) for 2 min: a) 40KC/60PV-T45-5R, b) 40KC/60PV-T45-10R, c) 40KC/60PV-T45-20R and d) 40KC/60PV-T45-30R.

4.4.10 pH-sensitivity of the films

The pH sensitivity of the prepared films was studied by immersing them in buffer solutions with varied pH values, ranging from 1 to 12. The pH responses of the films were observed in terms of color changing. Their digital photographs were

recorded and presented in Figure 4-21. The 40KC/60PV-T45-5R and 40KC/60PV-T45-10R exhibited soft pink color at pH 1-3. Increasing the environment pH values to 3-7 resulted in faded color of the film. When the solution pH was adjusted in the range of 8-11, the films responded and turned into greenish and finally changed to yellow at pH 12. The 40KC/60PV-T45-10R and 40KC/60PV-T45-20R displayed a deep shade of red at pH 1-2, light brown at pH 3-10, brownish-green colors at pH 11 and dark brown at pH 12. Among the samples loaded with different crude extract contents, the ones comprising 5 and 10% of the extract (40KC/60PV-T45-5R and 40KC/60PV-T45-10R) showed more obvious color change in respond to varied pH range and strong potential to be used as a pH indicator.

4.4.11 Colorimetric response of the pH sensitive films upon ammonia vapor

Colorimetric response of the fabricated films was evaluated under exposure to volatile of ammonia at different concentrations (1, 3 and 5% v/v) to investigate their sensitivity to alkaline gas. Color changes of the films at different periods of time were recorded by a digital camera and the photographs are displayed in Figure 4-22-4-27. The colorimetric response of all films was rapid. Within the first 2 min, their color changed to the shade of green that could be easily detected by naked eye. During 24 h of the test, the 40KC/60PV-T45-5R responded upon the basic volatile of 1, 3 and 5% ammonia solutions by changing from light green to bright yellow to greenish-yellow, while the 40KC/60PV-T45-10R, 40KC/60PV-T45-20R and 40KC/60PV-T45-30R films changed from light green to brownish yellow and light brown. Keeping the film in basic volatile environment more than 24 h did not significantly affect the film's color. For the films containing high extract content, the color changes were more clearly observed than those comprising lower extract content. The response of the films not only depended on the extract content but also on the concentration of ammonia. This colorimetric response was attributed to the diffusion of ammonia gas into the films, then hydrolyzed into hydroxyl ions and increased pH of the film comprising anthocyanin compounds. As a result, an alteration of anthocyanin chemical forms occurred in which the chalcone structure was predominant and contributed to brownish in color (Eze, Jayeoye, & Singh, 2022; Q. Wang et al., 2022).

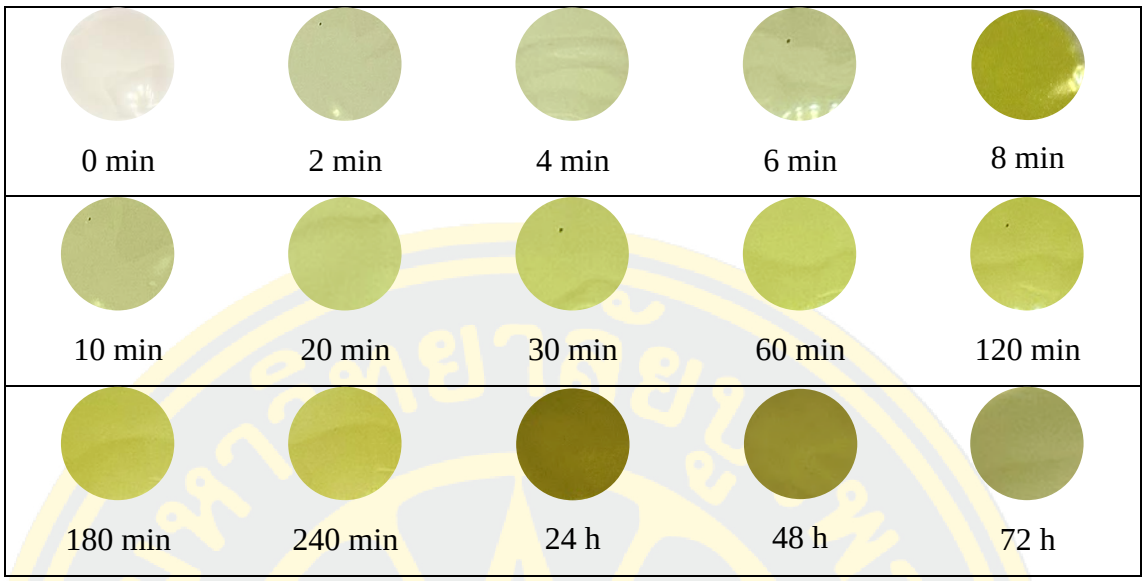

Figure 4-22 Digital photographs of the 40KC/60PV-T45-5R films exposed to volatile of 1%v/v ammonia solution at different time periods.

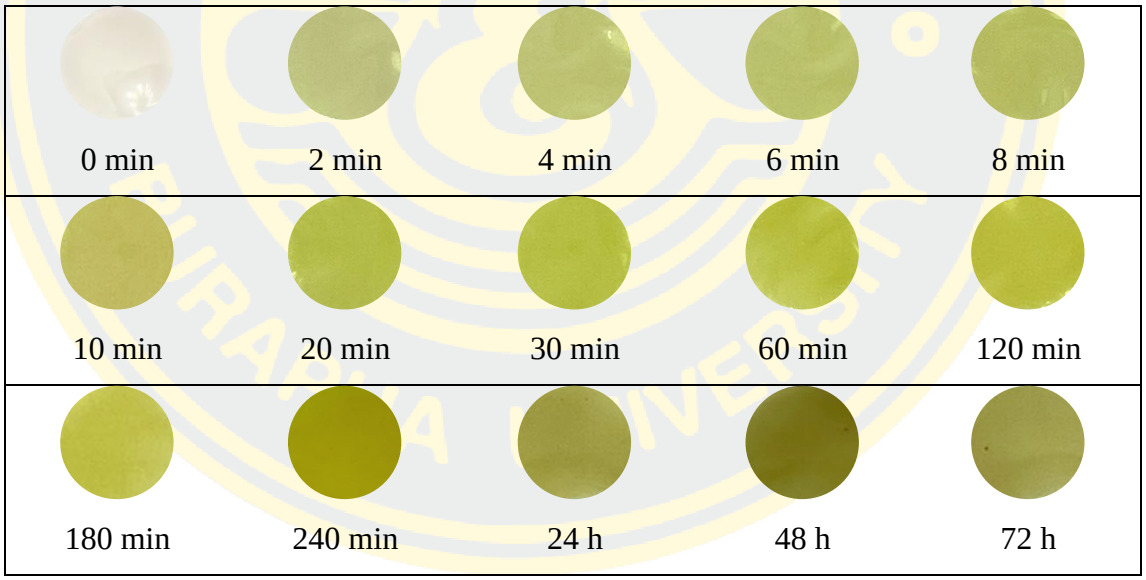

Figure 4-23 Digital photographs of the 40KC/60PV-T45-5R films exposed to volatile of 3%v/v ammonia solution at different time periods.

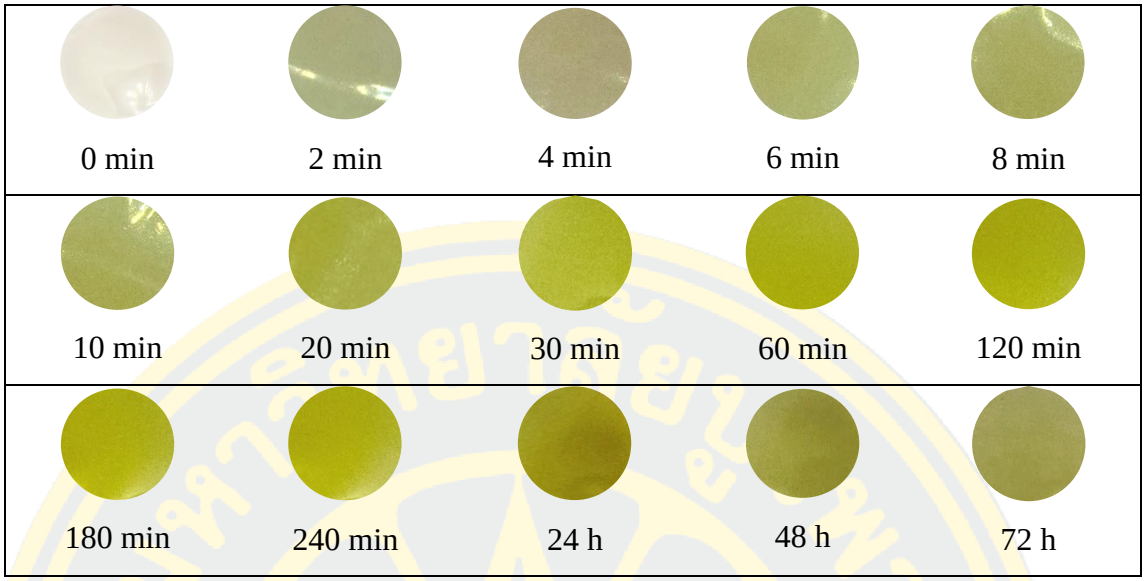

Figure 4-24 Digital photographs of the 40KC/60PV-T45-5R films exposed to volatile of 5%v/v ammonia solution at different time periods.

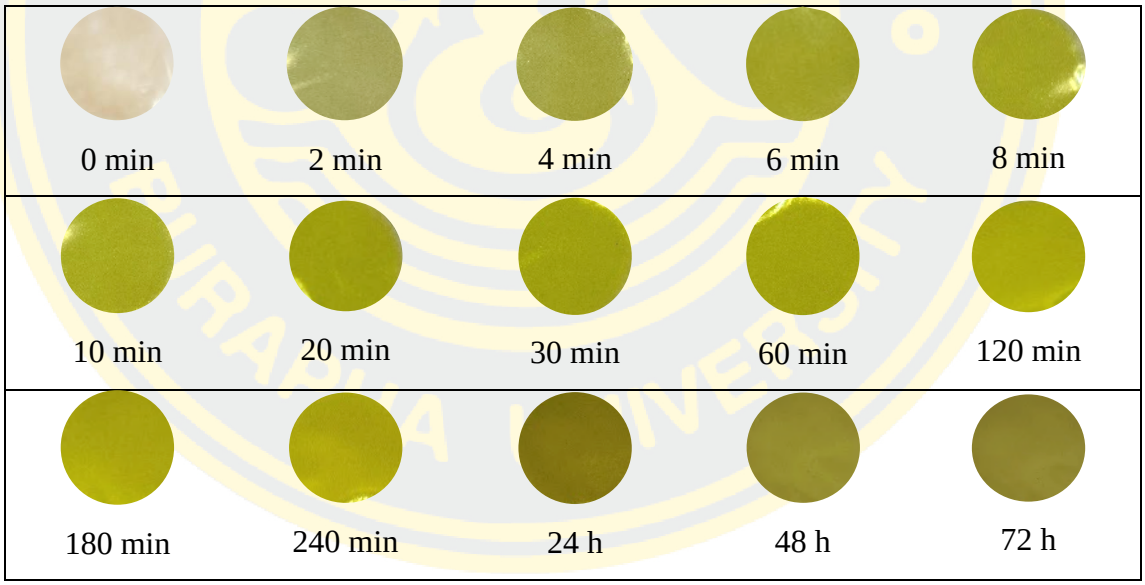

Figure 4-25 Digital photographs of the 40KC/60PV-T45-10R films exposed to volatile of 5%v/v ammonia solution at different time periods.

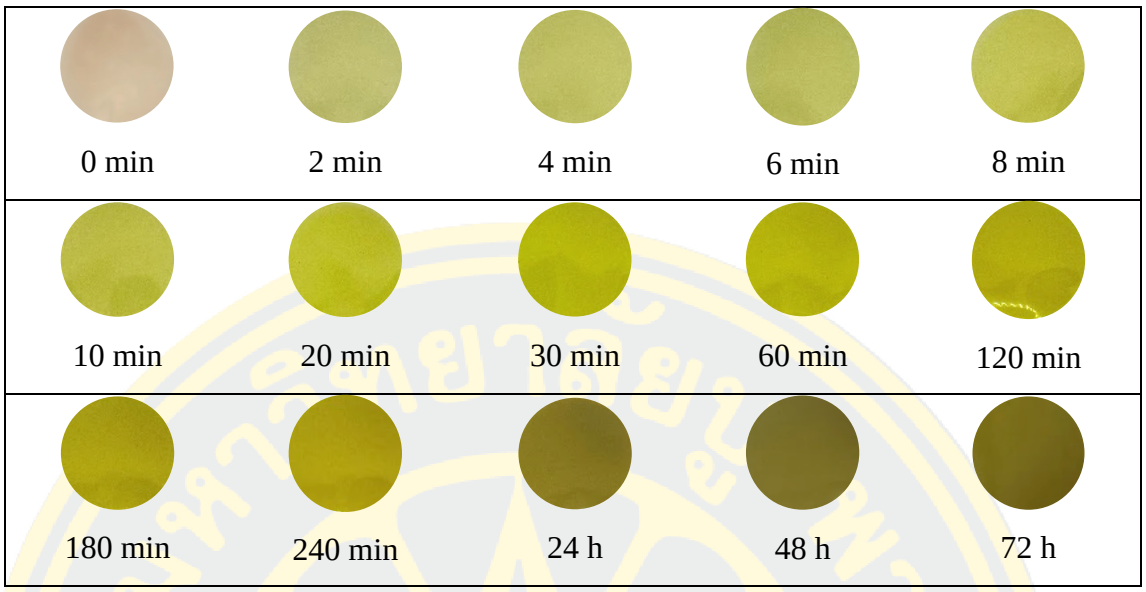

Figure 4-26 Digital photographs of the 40KC/60PV-T45-20R films exposed to volatile of 5%v/v ammonia solution at different time periods.

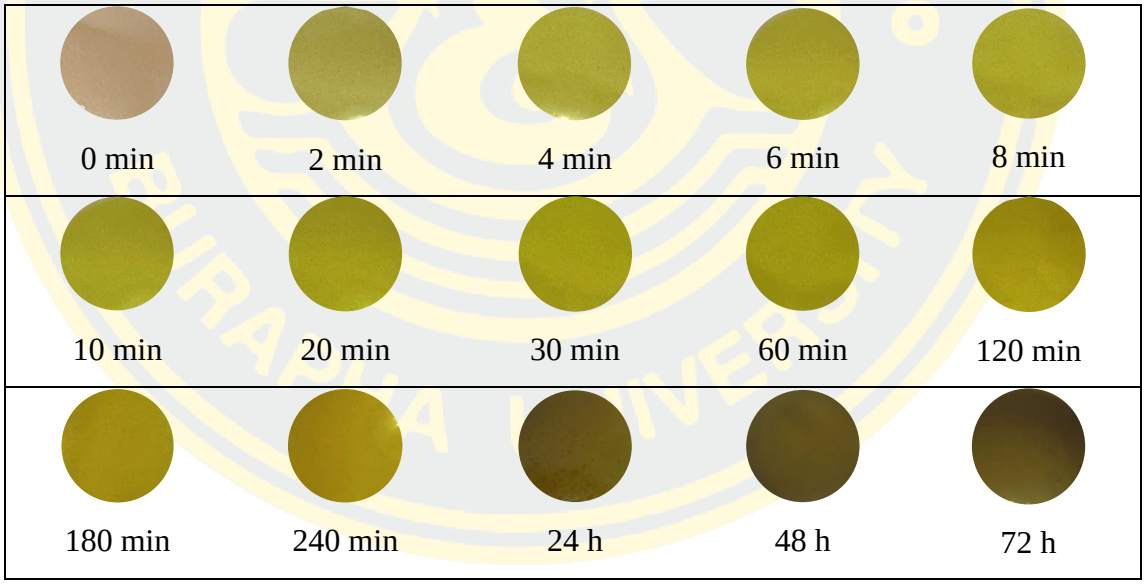

Figure 4-27 Digital photographs of the 40KC/60PV-T45-30R films exposed to volatile of 5%v/v ammonia solution at different time periods.

4.5 Application of the pH sensitive films for food freshness detection

4.5.1 Antioxidant ability

Antioxidant activity of the control and the pH-sensitive films was investigated by DPPH radical scavenging assay. As shown in Figure 4-34. The control sample showed slight antioxidant activity of 1.28%, probably due to the weak hydrogen-donating of κ-carrageenan (Y. Liu et al., 2020). With an incorporation of the crude extract, antioxidant activity of the films was enhanced along with the extract concentration. The 40KC/60PV-T45-5R containing low content (5%) of the crude extract showed the antioxidant activity of 4.39%. The other samples loaded with 10, 20 and 30% of the extract possessed 9.20, 17.6 and 27.2% of antioxidant activity. The improved antioxidant activity of the films was due to the abundant phenolic hydroxyl groups present in the structure of anthocyanins, which could scavenge free radicals by donating their phenolic hydrogen atoms (Amaregouda et al., 2022). The results suggested that the films containing the crude extract could be applied for an active food packaging material due to their advantage of antioxidant activity.

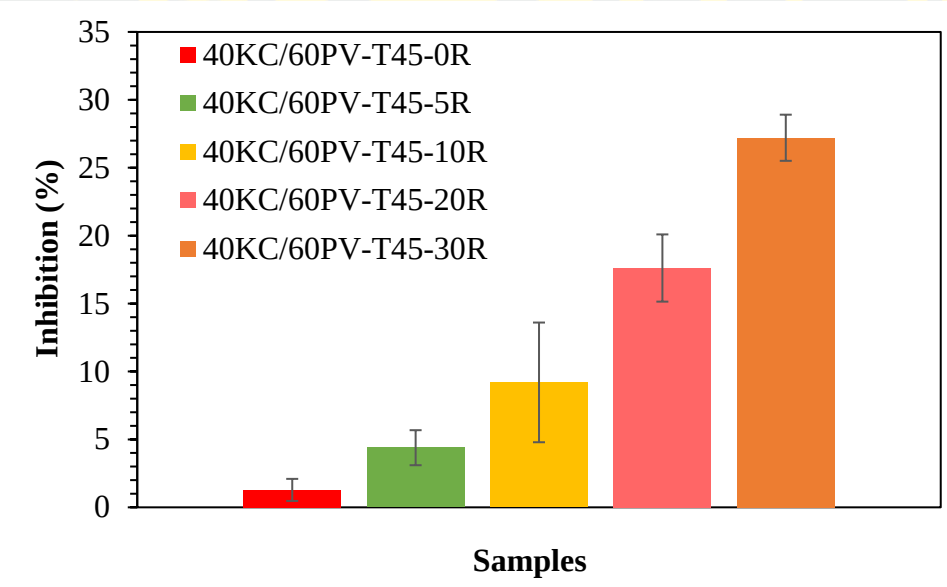

Figure 4-28 DPPH radical scavenging activity of the indicator films in DPPH

4.5.2 Color stability

Color stability of the indicator films was evaluated after storing them at room temperature for 28 days. The color change and the total color difference (ΔE) of the

films were monitored and the results are presented in Figure 4-35 and Table 4-7. From the digital photographs, color of all films during 28 days storage time was significantly unchanged under naked eye. Meanwhile, the total color difference (ΔE) values were slightly changes with increasing time. The ΔE values of 40KC/60PV-T45-5R and 40KC/60PV-T45-10R films were smaller than 5 over 28 days and the values of 40KC/60PV-T45-20R and 40KC/60PV-T45-30R films were gradually increased to 5.64 and 5.66, respectively. The results suggested the 40KC/60PV-T45-5R and 40KC/60PV-T45-10R films presented higher stability than the 40KC/60PV-T45-20R and 40KC/60PV-T45-30R films. This could be due to the slight degradation effect of anthocyanin when the storage time is prolonged. Similar results were also reported in the literature (Zheng, Liu, Yu, Farag, & Shao, 2023).

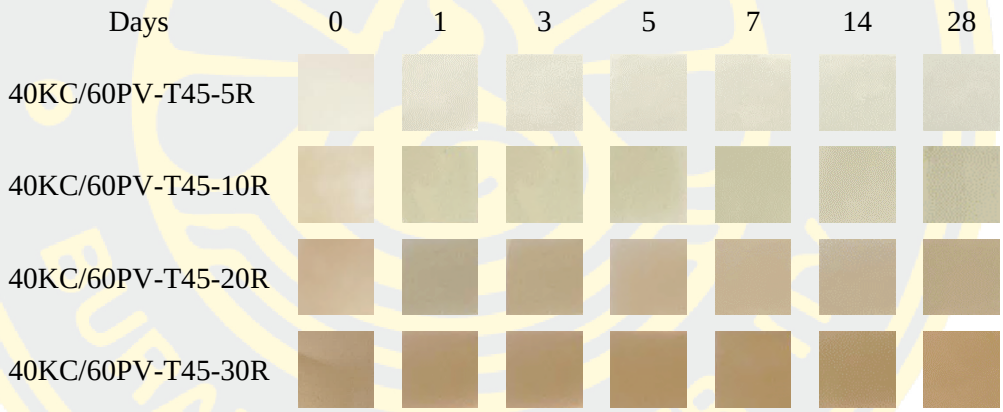

Figure 4-29 Digital photographs of indicator films after being stored for 28 days.

Table 4-7 Total color difference (ΔE) of the indicator films.

Samples	Days of storage					
	1	3	5	7	14	28
40KC/60PV-T45-5R	0.57	0.82	0.80	0.78	2.75	2.99
40KC/60PV-T45-10R	0.55	0.81	0.78	0.91	3.13	3.38
40KC/60PV-T45-20R	1.15	1.79	2.05	2.47	4.91	5.64
40KC/60PV-T45-30R	1.19	2.31	3.01	3.40	4.95	5.66

4.5.3 Application for food freshness detection

In general, protein-rich fresh food products, such as pork, chicken and shrimp, are decomposed by microbes and caused releasing of unpleasant gases including ammonia trimethylamine and dimethylamine, indicating food spoilage. The volatile ammonia would increase the pH value of the products from 5.8 to 7.8, resulting in a color change of the fabricated indicator films (Wu et al., 2021; Zheng et al., 2023). To investigate the efficacy of real-time detection, the fabricated films were applied to monitor the spoilage of shrimp. As shown in Figure 4-36, the colors of 40KC/60PV-T45-5R indicator film changed from pale yellow to green after 1 day of storage at room temperature in which the shrimp samples appeared orange, indicating spoilage of the product during storage. Apart from the naked eye detection, the colorimetric method was used to follow the changes of pH-sensitive film. The b parameter of the film changed from 8.79 ± 0.16 to 24.46 ± 0.26, and the ΔE values increased to 16.38 ± 0.23 after 1 day. (Table 4-8). These results suggested that the developed indicator film could be used to monitor food freshness during storage.

Table 4-8 Changes in color parameters of the indicator films during shrimp spoilage.

	Time (h)					
	0	4	8	24	48	72
Control						
L	93.66±0.06	93.69±0.09	92.30±0.01	93.63±0.04	93.32±0.54	92.81±0.71
a	-0.15±0.02	-0.11±0.03	-0.36±0.05	-0.14±0.00	-1.43±0.03	-1.49±0.05
b	1.60±0.03	1.49±0.02	1.25±0.03	1.56±0.05	1.35±0.06	1.59±0.15
ΔE	-	0.67±0.86	1.42±0.01	0.07±0.04	1.42±0.21	1.69±0.33
40KC/60PV-T45-5R						
L	85.92±0.12	85.87±0.01	84.12±0.14	82.78±0.19	82.91±0.70	72.51±0.13
a	0.41±0.05	-4.66±0.02	-5.68±0.02	-3.16±0.11	-1.76±0.24	1.34±0.02
b	8.79±0.16	18.32±0.03	25.66±0.05	24.46±0.26	18.36±0.39	20.11±0.12
ΔE	-	10.80±0.04	18.03±0.04	16.38±0.23	19.99±0.71	17.58±0.16

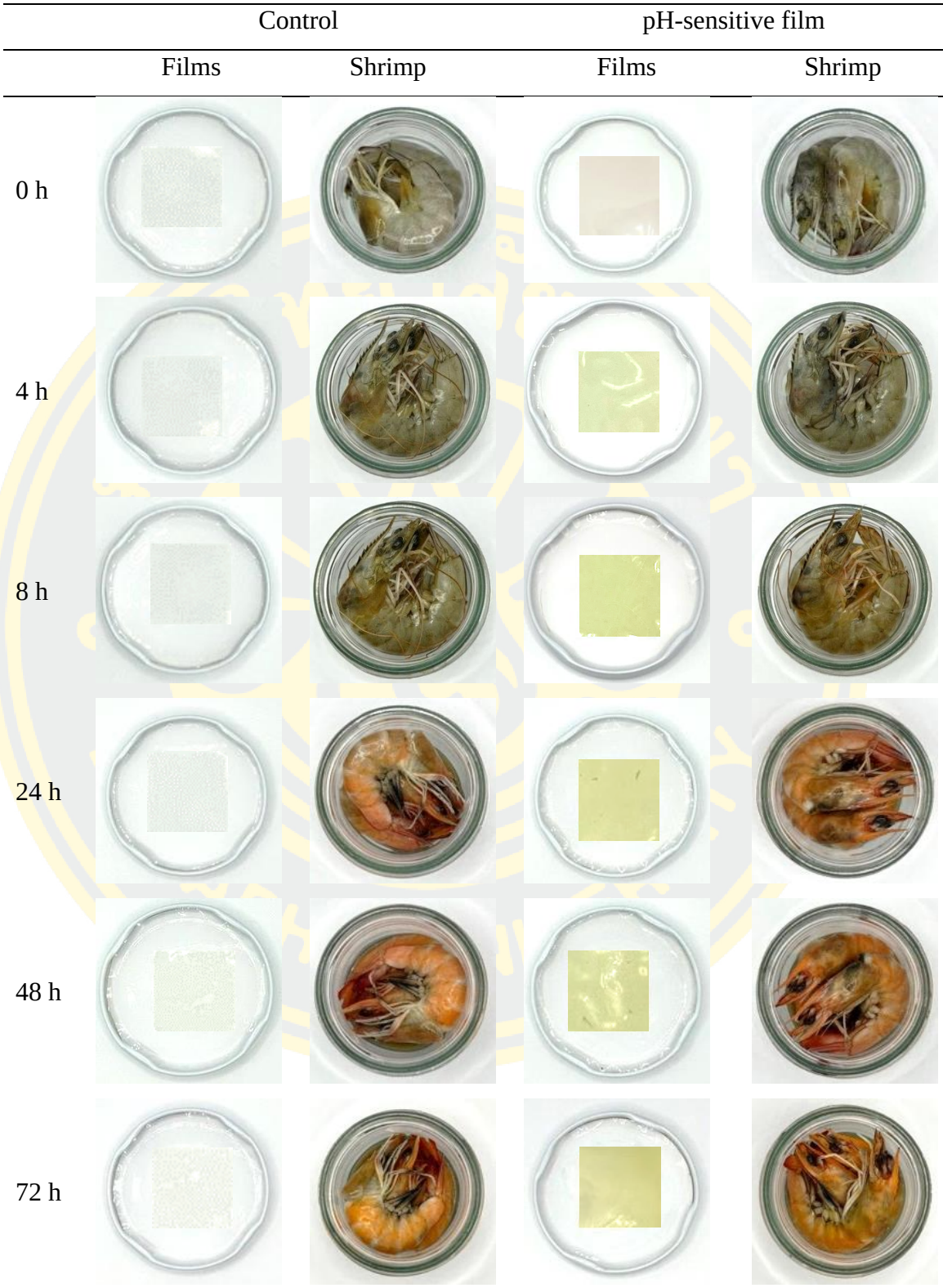

Figure 4-30 Application of the active 40KC/60PV-T45-5R film for monitoring the freshness of shrimp at room temperature.

CHAPTER 5
CONCLUSIONS

5.1 Preparation of the KC/PV and KC/PV-T films

The blend films of κ-carrageenan and poly(vinyl alcohol) at different ratios, 40KC/60PV, 50KC/50PV and 60KC/40PV, were successfully prepared using the solution casting method. All films were transparent and colorless. The incorporation of poly(vinyl alcohol) into the κ-carrageenan matrix improved the properties of the films. It was found that the film with a ratio of 40KC/60PV possessed decreased swelling, solubility, and moisture resistance. Additionally, tensile strength and elongation at break of this film were higher than those of the 50KC/50PV and 60KC/40PV. The 40KC/60PV was chosen for the optimization of physicochemical properties through organic-inorganic crosslinking via a sol-gel process. The sol-gel synthesis was successfully used to prepare the organic-inorganic films using TEOS as a crosslinker. The hybrid crosslinked 40KC/60PV-T45 films showed significantly improved mechanical properties and swelling ability. Therefore, the developed films demonstrated suitable properties for the application of packaging material.

5.2 Preparation of the pH-sensitive films

The anthocyanins extracted from the flowers of mexican petunia possess several benefits due to the presence of various bioactive compounds such as phenolics, *ortho*-hydroxyphenolics and anthocyanins. The crude extract displayed high antioxidant activity and pH-responsiveness, which showed strong potential for utilization in pH-sensitive films by adding the crude extract to the polymer matrix. Varied contents of crude extract were incorporated into the polymeric solution containing components for fabrication of the hybrid 40KC/60PV-T45 and were successfully formed into films using the sol-gel and solution casting processes.

All films demonstrated uniform surface morphology without phase separation. The presence of the crude extract greatly improved water resistance, thermal stability and UV barrier performance. Upon an incorporation of the crude extract, the pH-sensitive films showed an enhance in elongation at break while tensile strength at

break was decreased. In addition, the pH-sensitive films exhibited obvious color changes when exposed to volatile ammonia and when immersed in varying pH solutions. The pH-sensitive films underwent biodegradation in natural environment which was confirmed by the deterioration of surface morphology and the weight loss over 60 days of soil burial test. The results revealed that combination of κ-carrageenan/poly(vinyl alcohol) with anthocyanins extract was a good strategy to obtain packaging film that could be used as an efficient alternative for intelligent food packaging.

5.3 Application of the pH-sensitive films

The 40KC/60PV-T45-R films were developed comprising anthocyanin extract and investigated for food freshness monitoring using fresh shrimp as a food sample. The anthocyanin incorporated films displayed good sensitivity and color-respond upon shrimp spoilage. The active films demonstrated distinct color change under naked eye from pale yellow to green, corresponding to the real-time freshness quality of shrimp. Furthermore, the fabricated films incorporated with the crude extract possessed significant antioxidant activity that could be useful for the protection of packaged food. Shelf-life of the films in terms of color stability under naked eye was tested and confirmed no color change over 28 days. These results suggested that the developed pH-sensitive films could be successfully used as a real-time food freshness monitoring.

5.4 Recommendation

1. Further investigation on the capability of pH-sensitive films as a freshness indicator with various food samples.

2. Study on the quality of pH-sensitive films for freshness monitoring applications in food products under various conditions.

3. Investigation on mechanical properties of the film under different tests useful for packaging application such as impact and tear strength.

APPENDIX

1. Evaluation of total anthocyanin content using pH differential assay

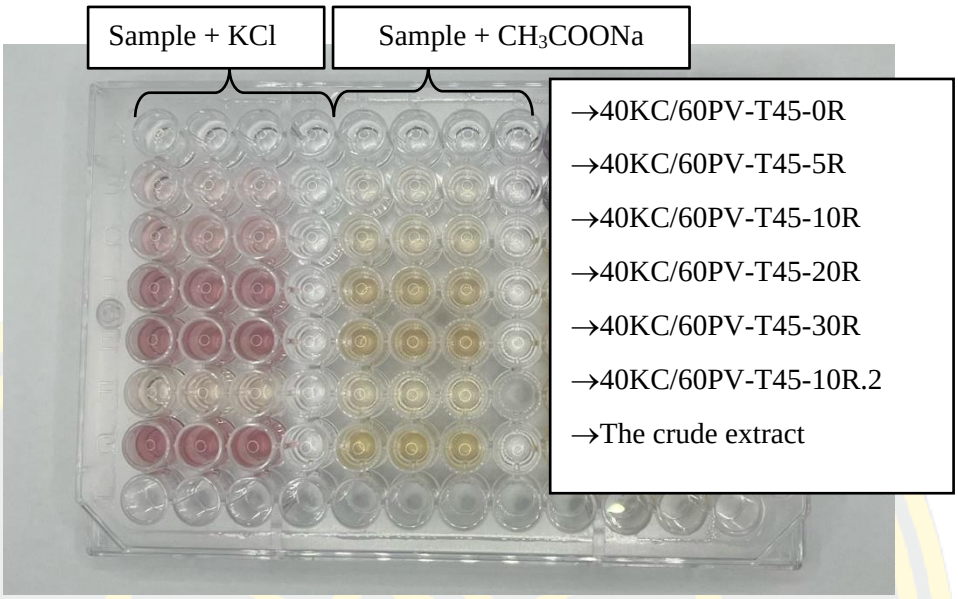

Figure A-1 Digital photograph of the sample determined with potassium chloride (KCl) and sodium acetate (CH_3COONa) solution.

2. Evaluation of antioxidant activity using DPPH assay.

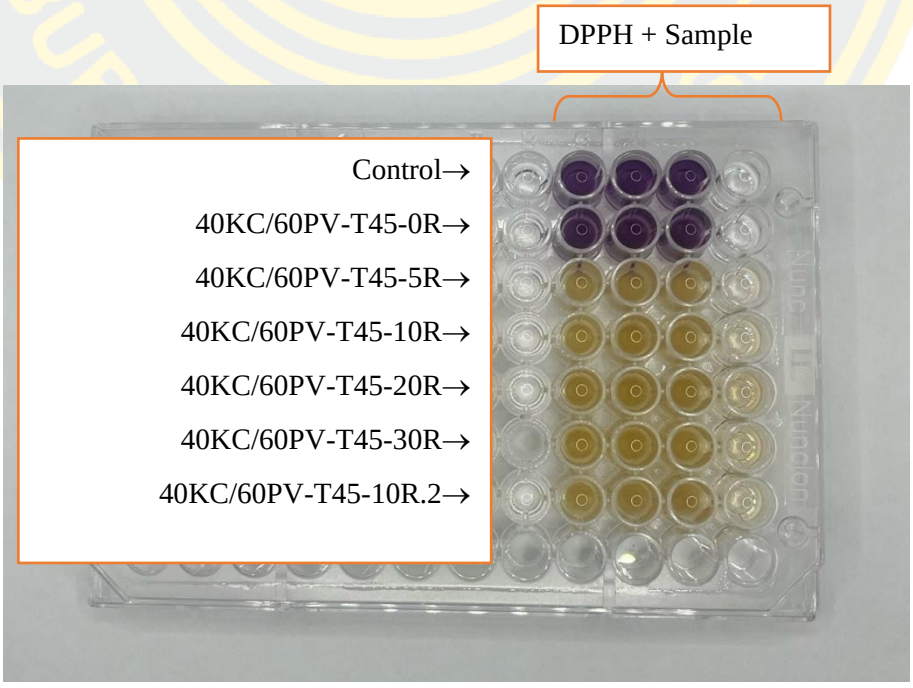

Figure A-2 Digital photograph of the sample determined using DPPH assay.

3. pH-sensitive ability.

Table A-1 Changes in color parameters of pH-sensitive films (40KC/60PV-T45-5R, 40KC/60PV-T45-10R) after immersion in different pH solutions (pH 1-12) for 2 min

pH	40KC/60PV-T45-5R				40KC/60PV-T45-10R			
	L	a	b	ΔE	L	a	b	ΔE
-	87.15	2.64	4.98	-	74.89	6.03	10.92	-
1	78.47	9.88	1.98	11.69	78.69	11.85	2.85	10.65
2	82.27	5.95	3.12	6.18	75.91	9.72	4.20	7.73
3	83.15	3.42	3.97	4.20	79.74	7.04	8.14	5.68
4	81.21	3.40	7.68	6.57	78.24	5.47	11.16	3.40
5	82.98	2.40	6.15	4.34	80.56	4.62	11.33	5.86
6	83.35	1.72	6.53	4.21	74.73	5.17	12.26	1.60
7	80.09	2.56	8.70	7.98	71.27	5.72	14.52	5.11
8	80.90	1.13	12.76	10.09	72.14	1.66	18.98	9.57
9	83.43	0.64	13.77	9.75	69.61	2.16	20.92	11.95
10	79.22	0.04	18.47	15.86	67.54	0.07	24.54	16.58
11	77.83	-0.12	20.88	18.64	64.79	0.78	23.45	16.93
12	72.77	4.28	34.54	32.91	69.79	7.33	40.23	29.78

Table A-2 Changes in color parameters of pH-sensitive films (40KC/60PV-T45-20R, 40KC/60PV-T45-30R) after immersion in different pH solutions (pH 1-12) for 2 min

pH	40KC/60PV-T45-20R				40KC/60PV-T45-30R			
	L	a	b	ΔE	L	a	b	ΔE
-	76.77	7.01	20.88	-	68.31	9.88	20.81	-
1	77.10	10.10	14.99	16.03	60.11	21.77	17.70	22.63
2	77.24	7.94	14.08	14.46	70.14	12.44	17.31	10.22
3	76.94	5.87	19.37	17.94	71.19	9.34	23.18	13.23
4	69.27	8.59	23.68	26.55	71.31	8.11	23.13	12.89
5	67.93	8.27	24.59	28.03	69.65	8.58	23.20	13.59
6	76.47	6.30	21.54	20.04	64.62	11.43	25.39	18.55
7	74.16	7.29	22.96	22.66	67.60	9.41	24.22	15.54
8	70.27	7.62	22.32	24.71	71.63	7.86	22.45	12.12
9	73.91	5.89	20.52	20.67	69.42	8.36	22.82	13.30
10	73.52	5.68	22.19	22.16	63.59	10.47	24.43	18.16
11	69.46	5.38	31.03	31.61	62.65	6.34	28.92	21.77
12	62.41	13.31	47.17	50.06	54.77	20.08	53.94	49.53

REFERENCES

Akhila, K., Sultana, A., Ramakanth, D., & Gaikwad, K. K. (2023). Monitoring freshness of chicken using intelligent pH indicator packaging film composed of polyvinyl alcohol/guar gum integrated with Ipomoea coccinea extract. *Food Bioscience, 52*. doi:10.1016/j.fbio.2023.102397

Akpan, U. G., & Hameed, B. H. (2010). The advancements in sol–gel method of doped-TiO2 photocatalysts. *Applied Catalysis A: General, 375*(1), 1-11. doi:10.1016/j.apcata.2009.12.023

Amaregouda, Y., Kamanna, K., & Gasti, T. (2022). Fabrication of intelligent/active films based on chitosan/polyvinyl alcohol matrices containing Jacaranda cuspidifolia anthocyanin for real-time monitoring of fish freshness. *Int J Biol Macromol, 218*, 799-815. doi:10.1016/j.ijbiomac.2022.07.174

Aslam, M., Kalyar, M. A., & Raza, Z. A. (2018). Polyvinyl alcohol: A review of research status and use of polyvinyl alcohol based nanocomposites. *Polymer Engineering & Science, 58*(12), 2119-2132. doi:10.1002/pen.24855

Athipornchai, A., & Jullapo, N. (2018). Tyrosinase inhibitory and antioxidant activities of Orchid (Dendrobium spp.). *South African Journal of Botany, 119*, 188-192. doi:10.1016/j.sajb.2018.09.003

Athipornchai, A., Kumpang, R., & Semsri, S. (2021). Potential Biological Activities of Clausena Essential Oils for the Treatment of Diabetes. *J Oleo Sci, 70*(11), 1669-1676. doi:10.5650/jos.ess19294

Balaji Ganesh, A., & Radhakrishnan, T. (2006). Estimation of Microbiologically Influenced Corrosion of Aluminium Alloy in Natural Aqueous Environment. *Nature and Science, 4*(3).

BeMiller, J. N. (2019). 13 – Carrageenans. *Carbohydrate Chemistry for Food Scientists (Third Edition)*, 279-291.

Ben Halima, N. (2016). Poly(vinyl alcohol): review of its promising applications and insights into biodegradation. *RSC Advances, 6*(46), 39823-39832. doi:10.1039/c6ra05742j

Biji, K. B., Ravishankar, C. N., Mohan, C. O., & Srinivasa Gopal, T. K. (2015). Smart packaging systems for food applications: a review. *Journal of food science and*

technology, 52(10), 6125-6135. doi:10.1007/s13197-015-1766-7

Bottom, R. (2008). Thermogravimetric analysis. *Principles and applications of thermal analysis, 1*(906), 87-118.

Campbell, D., Pethrick, R. A., & White, J. R. (2000). *Polymer Characterization: Physical Techniques, 2nd Edition*. CRC press.

Castañeda-Ovando, A., Pacheco-Hernández, M. d. L., Páez-Hernández, M. E., Rodríguez, J. A., & Galán-Vidal, C. A. (2009). Chemical studies of anthocyanins: A review. *Food Chemistry, 113*(4), 859-871. doi:10.1016/j.foodchem.2008.09.001

Chen, K., Li, J., Li, L., Wang, Y., Qin, Y., & Chen, H. (2023). A pH indicator film based on sodium alginate/gelatin and plum peel extract for monitoring the freshness of chicken. *Food Bioscience, 53*. doi:10.1016/j.fbio.2023.102584

Chianese, Angelo, J, H., Kramer, & eds. (2012). Industrial Crystallization Process Monitoring and Control. *Industrial crystallization process monitoring and control*.

Davis, J. R. (2004). *Tensile testing*: ASM international.

de Matos, M. F. R., Bezerra, P. Q. M., Correia, L. C. A., Viola, D. N., de Oliveira Rios, A., Druzian, J. I., & Nunes, I. L. (2021). Innovative methodological approach using CIELab and dye screening for chemometric classification and HPLC for the confirmation of dyes in cassava flour: A contribution to product quality control. *Food Chemistry, 365*, 130446.

Dille, M. J., Knutsen, S. H., & Draget, K. I. (2022). Gels and gelled emulsions prepared by acid-induced gelation of mixtures of faba bean (Vicia faba) protein concentrate and λ-carrageenan. *Applied Food Research, 2*(2). doi:10.1016/j.afres.2022.100174

Eze, F. N., Jayeoye, T. J., & Singh, S. (2022). Fabrication of intelligent pH-sensing films with antioxidant potential for monitoring shrimp freshness via the fortification of chitosan matrix with broken Riceberry phenolic extract. *Food Chem, 366*, 130574. doi:10.1016/j.foodchem.2021.130574

Farhat, H. (2021). *Operation, Maintenance, and Repair of Land-Based Gas Turbines*: Elsevier.

Forghani, S., Zeynali, F., Almasi, H., & Hamishehkar, H. (2022). Characterization of electrospun nanofibers and solvent-casted films based on Centaurea arvensis anthocyanin-loaded PVA/kappa-carrageenan and comparing their performance as colorimetric pH indicator. *Food Chem, 388*, 133057. doi:10.1016/j.foodchem.2022.133057

Fortunati, E., Luzi, F., Yang, W., Kenny, J. M., Torre, L., & Puglia, D. (2018). Bio-Based Nanocomposites in Food Packaging. In *Nanomaterials for food packaging* (pp. 71-110).

Freyre, R., Uzdevenes, C., Gu, L., & Quesenberry, K. H. (2015). Genetics and anthocyanin analysis of flower color in mexican petunia. *Journal of the American Society for Horticultural Science, 140*(1), 45-49.

Inacio, M. R., de Lima, K. M., Lopes, V. G., Pessoa, J. D., & de Almeida Teixeira, G. H. (2013). Total anthocyanin content determination in intact acai (Euterpe oleracea Mart.) and palmitero-jucara (Euterpe edulis Mart.) fruit using near infrared spectroscopy (NIR) and multivariate calibration. *Food Chem, 136*(3-4), 1160-1164. doi:10.1016/j.foodchem.2012.09.046

Ismail, W. N. W. (2016). Sol–gel technology for innovative fabric finishing—A Review. *Journal of sol-gel science and technology, 78*(3), 698-707. doi:10.1007/s10971-016-4027-y

Jamroz, E., Janik, M., Juszczak, L., Kruk, T., Kulawik, P., Szuwarzynski, M., . . . Khachatryan, K. (2021). Composite biopolymer films based on a polyelectrolyte complex of furcellaran and chitosan. *Carbohydr Polym, 274*, 118627. doi:10.1016/j.carbpol.2021.118627

JOSE MATHEW, S., & Francis, V. (2020). Development, Validation and Implementation of Universal Testing Machine. In.

Kanatt, S. R., Rao, M. S., Chawla, S. P., & Sharma, A. (2012). Active chitosan–polyvinyl alcohol films with natural extracts. *Food Hydrocolloids, 29*(2), 290-297. doi:10.1016/j.foodhyd.2012.03.005

Khan, A., Riahi, Z., Kim, J. T., & Rhim, J.-W. (2023). Gelatin/carrageenan-based smart packaging film integrated with Cu-metal organic framework for freshness monitoring and shelf-life extension of shrimp. *Food Hydrocolloids, 145*.

doi:10.1016/j.foodhyd.2023.109180

Korbag, I., & Mohamed Saleh, S. (2016). Studies on the formation of intermolecular interactions and structural characterization of polyvinyl alcohol/lignin film. *International Journal of Environmental Studies, 73*(2), 226-235. doi:10.1080/00207233.2016.1143700

Lapwanit, S., Sooksimuang, T., & Trakulsujaritchok, T. (2018). Adsorptive removal of cationic methylene blue dye by kappa-carrageenan/poly(glycidyl methacrylate) hydrogel beads: Preparation and characterization. *Journal of Environmental Chemical Engineering, 6*(5), 6221-6230. doi:10.1016/j.jece.2018.09.050

Li, L., Zhao, Z., Wei, S., Xu, K., Xia, J., Wu, Q., . . . Wang, L. (2024). Development and application of multifunctional films based on modified chitosan/gelatin polyelectrolyte complex for preservation and monitoring. *Food Hydrocolloids, 147*. doi:10.1016/j.foodhyd.2023.109336

Li, R., Wang, S., Feng, H., Zhuang, D., & Zhu, J. (2024). An intelligent chitosan/gelatin film via improving the anthocyanin-induced color recognition accuracy for beef sub-freshness differentiation monitoring. *Food Hydrocolloids, 146*. doi:10.1016/j.foodhyd.2023.109219

Liu, B., Zhang, J., & Guo, H. (2022). Research Progress of Polyvinyl Alcohol Water-Resistant Film Materials. *Membranes (Basel), 12*(3). doi:10.3390/membranes12030347

Liu, D., Cui, Z., Shang, M., & Zhong, Y. (2021). A colorimetric film based on polyvinyl alcohol/sodium carboxymethyl cellulose incorporated with red cabbage anthocyanin for monitoring pork freshness. *Food Packaging and Shelf Life, 28*. doi:10.1016/j.fpsl.2021.100641

Liu, J., Wang, H., Wang, P., Guo, M., Jiang, S., Li, X., & Jiang, S. (2018). Films based on κ-carrageenan incorporated with curcumin for freshness monitoring. *Food Hydrocolloids, 83*, 134-142. doi:10.1016/j.foodhyd.2018.05.012

Liu, Y., Qin, Y., Bai, R., Zhang, X., Yuan, L., & Liu, J. (2019). Preparation of pH-sensitive and antioxidant packaging films based on kappa-carrageenan and mulberry polyphenolic extract. *Int J Biol Macromol, 134*, 993-1001. doi:10.1016/j.ijbiomac.2019.05.175

Liu, Y., Zhang, X., Li, C., Qin, Y., Xiao, L., & Liu, J. (2020). Comparison of the structural, physical and functional properties of kappa-carrageenan films incorporated with pomegranate flesh and peel extracts. *Int J Biol Macromol, 147*, 1076-1088. doi:10.1016/j.ijbiomac.2019.10.075

Ly, B. C. K., Dyer, E. B., Feig, J. L., Chien, A. L., & Del Bino, S. (2020). Research Techniques Made Simple: Cutaneous Colorimetry: A Reliable Technique for Objective Skin Color Measurement. *J Invest Dermatol, 140*(1), 3-12 e11. doi:10.1016/j.jid.2019.11.003

Macdougall, D. B. (2010). Colour measurement of food: principles and practice. In *Colour Measurement* (pp. 312-342).

Menczel, J. D., & Prime, R. B. (2009). *Thermal analysis of polymers: fundamentals and applications*: John Wiley & Sons.

Meng, F., Zhang, Y., Xiong, Z., Wang, G., Li, F., & Zhang, L. (2018). Mechanical, hydrophobic and thermal properties of an organic-inorganic hybrid carrageenan-polyvinyl alcohol composite film. *Composites Part B: Engineering, 143*, 1-8. doi:10.1016/j.compositesb.2017.12.009

Miao, Y., Chen, Z., Zhang, J., Li, N., Wei, Z., Zhang, Y., . . . Zhang, J. (2023). Exopolysaccharide riclin and anthocyanin-based composite colorimetric indicator film for food freshness monitoring. *Carbohydr Polym, 314*, 120882. doi:10.1016/j.carbpol.2023.120882

Mohammed, A., & Abdullah, A. (2018). *Scanning electron microscopy (SEM): A review.* Paper presented at the Proceedings of the 2018 International Conference on Hydraulics and Pneumatics—HERVEX, Băile Govora, Romania.

Mok, C. F., Ching, Y. C., Muhamad, F., Abu Osman, N. A., Hai, N. D., & Che Hassan, C. R. (2020). Adsorption of Dyes Using Poly(vinyl alcohol) (PVA) and PVA-Based Polymer Composite Adsorbents: A Review. *Journal of Polymers and the Environment, 28*(3), 775-793. doi:10.1007/s10924-020-01656-4

Moradi, M., Tajik, H., Almasi, H., Forough, M., & Ezati, P. (2019). A novel pH-sensing indicator based on bacterial cellulose nanofibers and black carrot anthocyanins for monitoring fish freshness. *Carbohydr Polym, 222*, 115030. doi:10.1016/j.carbpol.2019.115030

Muppalaneni, s. (2013). Polyvinyl Alcohol in Medicine and Pharmacy: A Perspective. *Journal of Developing Drugs, 02*(03). doi:10.4172/2329-6631.1000112

Nagarkar, R., & Patel, J. (2019). Polyvinyl alcohol: A comprehensive study. *Acta Sci. Pharm. Sci, 3*(4), 34-44.

Otles, S., & Yalcin, B. (2008). Intelligent food packaging. *LogForum, 4*(4).

Park, S. Y., Lee, B. I., Jung, S. T., & Park, H. J. (2001). Biopolymer composite films based on k-carrageenan and chitosan. *Materials Research Bulletin, 36*, 511-519.

Peralta, J., Bitencourt-Cervi, C. M., Maciel, V. B. V., Yoshida, C. M. P., & Carvalho, R. A. (2019). Aqueous hibiscus extract as a potential natural pH indicator incorporated in natural polymeric films. *Food Packaging and Shelf Life, 19*, 47-55. doi:10.1016/j.fpsl.2018.11.017

Pierre, A. C. (2020). *Introduction to sol-gel processing*. Springer Nature.

Pipattanawarothai, A., & Trakulsujaritchok, T. (2020). Hybrid polymeric chemosensor bearing rhodamine derivative prepared by sol-gel technique for selective detection of Fe3+ ion. *Dyes and Pigments, 173*. doi:10.1016/j.dyepig.2019.107946

Praseptiangga, D., Mufida, N., Panatarani, C., & Joni, I. M. (2021). Enhanced multi functionality of semi-refined iota carrageenan as food packaging material by incorporating SiO2 and ZnO nanoparticles. *Heliyon, 7*(5), e06963. doi:10.1016/j.heliyon.2021.e06963

Qin, Y., Liu, Y., Zhang, X., & Liu, J. (2020). Development of active and intelligent packaging by incorporating betalains from red pitaya (Hylocereus polyrhizus) peel into starch/polyvinyl alcohol films. *Food Hydrocolloids, 100*. doi:10.1016/j.foodhyd.2019.105410

Roy, N., Saha, N., Kitano, T., & Saha, P. (2012). Biodegradation of PVP-CMC hydrogel film: a useful food packaging material. *Carbohydr Polym, 89*(2), 346-353. doi:10.1016/j.carbpol.2012.03.008

Santos, M. C. D., Morais, C. L. M., & Lima, K. M. G. (2021). ATR-FTIR spectroscopy for virus identification: A powerful alternative. *Biomedical Spectroscopy and Imaging, 9*(3-4), 103-118. doi:10.3233/bsi-200203

Schaefer, D., & Cheung, W. M. (2018). Smart Packaging Opportunities and Challenges.

Procedia Cirp, 72, 1022–1027.

Sedayu, B. B., Cran, M. J., & Bigger, S. W. (2019). A Review of Property Enhancement Techniques for Carrageenan-based Films and Coatings. *Carbohydr Polym, 216*, 287-302. doi:10.1016/j.carbpol.2019.04.021

Sharma, S., Barkauskaite, S., Jaiswal, A. K., & Jaiswal, S. (2021). Essential oils as additives in active food packaging. *Food Chem, 343*, 128403. doi:10.1016/j.foodchem.2020.128403

Shen, Y.-R., & Kuo, M. I. (2017). Effects of different carrageenan types on the rheological and water-holding properties of tofu. *Lwt, 78*, 122-128. doi:10.1016/j.lwt.2016.12.038

Sianturi, G. L. R., Trisnawati, E. W., Koketsu, M., & Suryanti, V. (2023). Chemical constituents and antioxidant activity of Britton's wild petunia (Ruellia brittoniana) flower. *Biodiversitas Journal of Biological Diversity, 24*(7). doi:10.13057/biodiv/d240703

Singh, S., Nwabor, O. F., Syukri, D. M., & Voravuthikunchai, S. P. (2021). Chitosan-poly(vinyl alcohol) intelligent films fortified with anthocyanins isolated from Clitoria ternatea and Carissa carandas for monitoring beverage freshness. *Int J Biol Macromol, 182*, 1015-1025. doi:10.1016/j.ijbiomac.2021.04.027

Sobhan, A., Muthukumarappan, K., & Wei, L. (2022). A biopolymer-based pH indicator film for visually monitoring beef and fish spoilage. *Food Bioscience, 46*. doi:10.1016/j.fbio.2021.101523

Sukhlaaied, W., & Riyajan, S. A. (2013). Synthesis and properties of carrageenan grafted copolymer with poly(vinyl alcohol). *Carbohydr Polym, 98*(1), 677-685. doi:10.1016/j.carbpol.2013.06.047

Supalert, P., Meelapsom, R., Prakobkij, A., Supasorn, S., & Jarujamrus, P. (2021). Acid– Base Titration Based on Microfluidic Paper–Based Analytical Device (μPAD) Using Natural Indicator. *Journal of Research Unit on Science, Technology and Environment for Learning,, 12*(2), 186-201.

Trakulsujaritchok, T., & Suksai, C. (2018). Sensor for heavy metal ions in aqueous media based on poly(vinyl alcohol)/silical hybrid material synthesized by sol-gel method. *Research Grant of Burapha University*.

Tursunov, O., Dobrowolski, J., Klima, K., Kordon, B., Ryczkowski, J., Tylko, G., & Czerski, G. (2015). The Influence of Laser Biotechnology on Energetic Value and Chemical Parameters of Rose Multiflora Biomass and Role of Catalysts for bio-energy production from Biomass: Case Study in Krakow-Poland. *Science and Education Publishing, 3*(2), 58-66. doi:10.12691/wjee-3-2-5

Wang, Q., Jiang, Y., Chen, W., Julian McClements, D., Ma, C., Liu, X., & Liu, F. (2022). Development of pH-responsive active film materials based on purple corncob and its application in meat freshness monitoring. *Food Res Int, 161*, 111832. doi:10.1016/j.foodres.2022.111832

Wang, S., Ren, J., Li, W., Sun, R., & Liu, S. (2014). Properties of polyvinyl alcohol/xylan composite films with citric acid. *Carbohydr Polym, 103*, 94-99. doi:10.1016/j.carbpol.2013.12.030

Wu, L. T., Tsai, I. L., Ho, Y. C., Hang, Y. H., Lin, C., Tsai, M. L., & Mi, F. L. (2021). Active and intelligent gellan gum-based packaging films for controlling anthocyanins release and monitoring food freshness. *Carbohydr Polym, 254*, 117410. doi:10.1016/j.carbpol.2020.117410

Yong, H., Wang, X., Bai, R., Miao, Z., Zhang, X., & Liu, J. (2019). Development of antioxidant and intelligent pH-sensing packaging films by incorporating purple-fleshed sweet potato extract into chitosan matrix. *Food Hydrocolloids, 90*, 216-224. doi:10.1016/j.foodhyd.2018.12.015

Zakaria, Z., Kamarudin, S. K., Kudus, M. H. A., & Wahid, K. A. A. (2022). κ-carrageenan/polyvinyl alcohol-graphene oxide biopolymer composite membrane for application of air-breathing passive direct ethanol fuel cells. *Journal of Applied Polymer Science, 139*(22). doi:10.1002/app.52256

Zhang, X., Liu, Y., Yong, H., Qin, Y., Liu, J., & Liu, J. (2019). Development of multifunctional food packaging films based on chitosan, TiO2 nanoparticles and anthocyanin-rich black plum peel extract. *Food Hydrocolloids, 94*, 80-92. doi:10.1016/j.foodhyd.2019.03.009

Zhao, L., Liu, Y., Zhao, L., & Wang, Y. (2022). Anthocyanin-based pH-sensitive smart packaging films for monitoring food freshness. *Journal of Agriculture and Food Research, 9*. doi:10.1016/j.jafr.2022.100340

Zheng, L., Liu, L., Yu, J., Farag, M. A., & Shao, P. (2023). Intelligent starch/chitosan-based film incorporated by anthocyanin-encapsulated amylopectin nanoparticles with high stability for food freshness monitoring. *Food Control, 151*. doi:10.1016/j.foodcont.2023.109798